R. & M. No. 3802

PROCUREMENT EXECUTIVE MINISTRY OF DEFENCE

AERONAUTICAL RESEARCH COUNCIL
REPORTS AND MEMORANDA

A Gust Tunnel Facility

By M. H. PATEL AND G. J. HANCOCK
Queen Mary College, University of London

LONDON: HER MAJESTY'S STATIONERY OFFICE
1977
£5 net

A Gust Tunnel Facility

By M. H. PATEL AND G. J. HANCOCK
Queen Mary College, University of London

Reports and Memoranda No. 3802*
June, 1976

Summary

A gust tunnel, which has been under development in the Aeronautical Department of Queen Mary College since 1965, is fully described. Extensive information on the hardware and apparatus associated with the tunnel is followed by an account of its steady and oscillatory flow characteristics. These latter are described for single frequencies as well as at combinations of two frequencies. The generation of non-periodic transient gusts is also reported together with brief reviews of past experimental research that has been conducted with the facility.

* Replaces A.R.C. 36 933

LIST OF CONTENTS

1. Introduction

A large number of current aerodynamic problems in both the aeronautical and non-aeronautical industries involve the fluid mechanics of unsteady flows. The main areas of interest include the role of freestream unsteadiness in fundamental phenomena such as boundary layer stability and transition to turbulence, unsteady boundary layer development, flow separation, vortex shedding from bluff bodies as well as the dynamic problem associated with the response of bodies to unsteady flow conditions; the motion of aircraft in disturbed flight due to atmospheric turbulence comes into the latter category. Wind tunnel investigations play an invaluable role in the development of our understanding of such flows. It is common practice to investigate unsteady problems by oscillating models in a conventional wind tunnel. However, there are situations whereby it is more convenient to have a stationary model in a non-conventional wind tunnel in which the tunnel flow is basically oscillatory or unsteady. It is with the latter type of tunnel that our report is concerned.

Several wind tunnels have been built over the past years to produce various unsteady or gust type flows.

Two notable facilities have been developed at Langley Research Centre, U.S.A., primarily for producing vertical oscillatory gusts superimposed on a uniform stream. Both facilities utilise the vertical velocity component of a trailing vortex wake shed by an oscillating pair of low aspect ratio half-wings situated ahead of the working section. The first facility, a low speed one described by Reid and Wrestler[1] used a pair of oscillating half-wings on one sidewall just aft of the contraction with the test half-model on the opposite sidewall in the closed test section. The second facility, as described by Gilman and Bennett,[2] in the 4·88 m (16 ft) square transonic tunnel, had two oscillating half-wings on each sidewall at the downstream end of the contraction so that a complete model could be mounted on the tunnel centre-line in the closed test section. Both facilities were capable of producing harmonic gusts of adequate amplitude at low frequencies; however, the available amplitude decreased with increasing frequency to a negligible level at a frequency parameter (ω/U_0) of approximately 1·15 per metre. The zones of uniform gust conditions were small compared to the working section area.

Reid and Wrestler report the results of low speed tests on a half-model of a delta wing of 60 degrees leading edge sweep. In the transonic facility, the dynamic responses of free flight models on soft suspensions were measured in oscillatory flow using both air and freon as working mediums.

A novel method of generating ramp gusts was developed by Schetzer[3]. A 'ramp like' variation of vertical velocity at the test section was produced by the downstream motion of a bump along the working section floor. The gradient of the ramp could be controlled by varying the ratio of bump speed to tunnel air speed. Gust angles of as high as 12 degrees were reported by Schetzer together with some results of the lift response of a two-dimensional aerofoil under these flow conditions.

Vertical velocity variations can be superimposed on a wind tunnel flow by the installation of a set of linked and closely spaced parallel aerofoils (a 'venetian blind') at the flow inlet to an open working section. Pitching motion of the paralleled array of aerofoils imparts corresponding vertical velocities in the downstream flow. Oscillatory, ramp and even random (two dimensional) gusts can be produced by suitable pitching motion of the aerofoil array. The downstream flow in the test section has a high turbulence level due to the mixing of the aerofoil wakes. One advantage of this arrangement is that it is capable of producing sharp edged gusts when the aerofoil array is moved impulsively. Several of these facilities have been built. Schetzer[3] at Michigan University, Sawyer[4] at Salford University in Britain and Hirosue *et al.*[5] in Japan.

Bicknell and Parker[6] describe the preliminary study of a similar gust generation mechanism employing oscillating flaps on a pair of large chord aerofoils mounted just inside the wind tunnel exit nozzle. The results are encouraging with uniform sinusoidal gusts of large amplitude being generated between the aerofoil wakes in the semi-open working section although the capability for producing sharp edged gusts is degraded in comparison with that of the 'venetian blind' arrangement.

In a gust facility developed at the R.A.E. by Hunt, Roberts and Walker[7] delta-wing models were mounted on a sledge which was propelled down a straight track and through the open jet from a low speed tunnel transverse to the track. The authors report transient lift and pressure measurements on a delta wing of aspect ratio 1·2.

A recently developed gust facility at Cambridge University has been described by Horlock[8]. It consists of a low speed wind tunnel (0·69 m by 0·46 m) in which a travelling wave type of oscillatory gust flow is generated by a travelling wave motion of the upper and lower walls of the test section. Because of engineering limitations, the travelling wave velocities are considerably less than typical freestream mean velocities. Both transverse and streamwise gusts can be obtained by moving the upper and lower wall waves either in phase or 180 degrees out of phase relative to each other. The tunnel has been used for testing isolated and cascade aerofoils in transverse gusts at low frequency parameters (Satyanarayana *et al.*[9]).

The gust tunnel developed in the Aeronautical Department at Queen Mary College is based on the requirement to produce a wide range of gust conditions in a relatively large working section while retaining an essentially irrotational flow field. The gust facility has been under development and in use since 1965. It is based on a straight through wind tunnel (Fig. 1) being built in the department at the time. Unsteady flows in the working section are generated by the up and down tilting motion of a flexible nozzle at the exit to the contraction. Any movement of the nozzle perturbs shear layers at the top and bottom of a semi-open working section causing them to deform into concentrated vortices in the mixing regions of the jet. These vortices convect downstream and induce a travelling wave type of unsteadiness in the potential core of the jet. Various oscillatory and non-periodic gusts can be induced in the working section flow by varying the nozzle input disturbance. In particular, oscillatory harmonic gusts of adequate amplitude can be generated over a frequency range of 2 to 12 Hz.

The gust tunnel is described in detail in subsequent Sections; Section 2 describes the tunnel hardware and Section 3 gives the operative flow mechanism and the characteristics of the various gust flows that are available. Some experimental investigations are briefly reviewed in Section 4 and finally Section 5 summarises significant details concerning the calibration and use of the tunnel.

2. The Facility and Associated Apparatus

2.1. Wind Tunnel and Ancillary Equipment

The basis of the facility is a blow through wind tunnel (Fig. 1) 'wrapped' round the laboratory floor with the motor section in the basement and the settling chamber and contraction on the ground floor. The tunnel flow is turned round the laboratory floor by a series of expanded grids and led into the settling chamber which incorporates three wire gauze screens. A high contraction area ratio of 14·5 : 1 leads to a rectangular exit 0·76 m (30 in) high and 0·99 m (39 in) across. A 22·5 kW (30 H.P.) electric motor provides a continuously variable speed of up to 30 m/s in the working section.

An unsteady flow is superimposed on the freestream by the motion of flexible extensions at the top and bottom of the exit to the contraction. As shown in Fig. 2, these flexible plates are attached to the contraction at one end and to an aluminium frame at the other. This frame can be displaced up or down by a hydraulic actuator giving a flexible nozzle which can be tilted through an angle, to the horizontal, of ±5 degrees corresponding to a frame travel of 6·6 cm. The sidewall extensions in the nozzle are kept stationary.

The flexible extensions are aluminium plates with a graded stiffness along their length such that most of the bending occurs near to the end fixed to the contraction; the rest of the plates remain almost straight and parallel to each other. Plate I shows an end-on view of the nozzle and actuator mechanism.

The working section has solid side-walls and 'slotted' upper and lower walls which are positioned as shown in Fig. 3(i). These 'slotted' walls are made up of reinforced flat plates with a large number of regularly spaced openings (Fig. 3(ii)). The walls, with their small inclination to the flow direction, are necessary to smoothly damp down the rapid increase in gust angle with distance downstream which is a feature of the gust mechanism—*see* Section 3.2 for more details. Both the upper and lower walls are identical except for a 5 cm wide slit running down the centreline of the upper wall to provide access into the flow for traverse gears and model mounting rigs. The working section framework, primarily designed for its rigidity, is built up of 7·6 cm square steel box sections. Wooden side-walls with three pairs of ports for model mounting and a pair of large observation windows complete the structure. When the section is in use, it is bolted to the laboratory floor with the front end close to but not in contact with the movable nozzle. In this way, no mechanical vibrations induced by motion of the nozzle can be transmitted directly to the models under test.

The working section is fitted with an integral motorised traverse gear to enable automatic positioning and traversing of sensor probes within the flow. The traverse gear provides probe motion along all three axes (defined in Fig. 3(i)) with a positioning accuracy of ±0·5 mm along each axis. Such accuracy is adequate for tunnel calibration and overall flow investigations. For more precise displacement measurements, a selection of very accurate gears of limited traverse range are also available.

The mounting of wings, aircraft models, etc., on their force-measuring stings is accomplished by a variable incidence sting support rig. As shown in Fig. 4, the rig consists of a lever system incorporating two parallel streamlined steel bars which allow the test model to vary its incidence about a chosen point relative to it. The lever system is connected to a variable speed electric motor which can select a sting incidence of up to ±20 degrees. Automatic readings of the model attitude are derived from a rotary potentiometer fitted to the driving motor. Three pairs of ports on the tunnel sidewalls are also available for mounting two dimensional and half models.

2.2. The Nozzle Motion System

The aluminium frame to which the flexible nozzle plates are attached is linked to an electro-hydraulic servo-mechanism originally built by Fairey Surveys Ltd. This mechanism is capable of producing a displacement of the frame which can follow a time dependent input voltage signal accurately over a limited frequency range (up to about 20 Hz). The maximum available movement in the mechanism is 7·62 cm at low frequencies, decreasing to less than 0·5 cm at higher frequencies (over 20 Hz). An oil pressure supply of 21 MN/m^2 (3000 p.s.i.) is ducted to a double-sided piston in the actuator unit by a system of two electro-hydraulic servo-valves which control the flow of oil to either side of the piston causing it to move up or down. An integral electro-magnetic displacement transducer, which is connected between the piston and main body of the actuator, provides a feedback signal through a d.c. coupled amplifier to the servo-valves, tending to reduce the difference between the transducer and input voltages. The actuator thus produces a displacement which closely follows the input signal. The transducer output is also used to indicate the actual frame displacement. Fig. 5 shows the calibration plot of the displacement transducer output against nozzle angle which is defined as the angle to the horizontal subtended by the moving frame about the exit to the contraction which is 0·38 m aft of the nozzle frame.

The linkage between the nozzle frame and servo-mechanism (Fig. 6) is made up of two sections which perform separate functions. The first section is in the form of a steel rod notched in two places and designed primarily to take up the small horizontal movements of the nozzle frame that will occur. The second section consists of a push-rod which provides some measure of protection for the nozzle in an emergency. This push-rod is made up of two concentric rods which are held together by two shear pins 3·18 mm in diameter. Excessive loads due to a runaway failure of the actuation system would be isolated from the flexible nozzle by breakage of the shear pins.

A balancing mechanism, shown in Fig. 7, is also incorporated in the actuator system to prevent vibrations being transmitted to the laboratory floor. The mass of the frame and the moving parts of the actuator are counterbalanced by two large masses through a pivot and lever on each side of the actuator. A 20:1 mechanical advantage on the levers does require large masses for counterbalance but it also minimises reaction forces on the ball bearing lever pivots.

Input voltages to the actuator mechanism are supplied by either a step and ramp voltage source (Servomex Controls Ltd. Waveform Generator type LF51) or by a Muirhead D880B decade oscillator for harmonic input voltages at a signal frequency.

For a combination input of two frequencies, the sum of signals from separate oscillators could not be used because the inevitable small difference in the time scales of the two oscillators causes a continuous phase change between the added components at the two frequencies. This difficulty is circumvented by taking just one oscillatory signal and using a digital divider to obtain a square wave with a frequency which is equal to the input frequency divided by any pre-selected integer between 2 and 16. The divided square wave is filtered to give a sinusoidal signal which is then added to the original input to give a signal made up of two frequencies. The fact that the upper frequency divided by the lower frequency has to be an integer between 2 and 16 imposes some limitations on the possible combinations available for nozzle excitation. As shown in Fig. 8, provision is made for changing the phase between two constituent frequencies as well as for altering their individual amplitudes in the final input signal for the actuator mechanism.

2.3. Sensors

Measurement of forces, pressures, velocities and flow angles in unsteady flows require instruments with fast response times. There is no difficulty with most conventional wind tunnel instrumentation such as strain-gauged sting balances, strain-gauged pressure transducers and single hot wire anemometers.

Additionally, an accurate sensor of instantaneous flow angle is required for the two-dimensional (constant with y) gust flows available in the tunnel. Pressure tube yawmeters suffer from lag and attentuation in the connecting tubes. Inclined pairs of hot wires tend to display nonlinearities and interference effects between the adjacent wire elements and they are difficult to use. A suitable flow angle meter with good linearity and a fast response is obtained by using a simple small 10 percent thick rectangular wing (12·7 × 50·8 mm) on a strain-gauged sting as shown in Fig. 9(i).

This rectangular wing is made from solid aluminium with a smooth symmetrical aerofoil shape in cross-section. Two Endevco 1100 Series 'Pixie' semiconductor strain gauge beams are used as two arms of a Wheatstone bridge circuit which provides a high output that is measurable directly without amplification. The sting-wing natural frequency is approximately 200 Hz and thus well separated from the frequencies over which experiments are carried out.

Figs. 9 also illustrate a typical static calibration as well as the bridge circuit. The output voltage (V) is linearly dependent on angle of incidence (α) within a range $-4° < \alpha < 4°$ and on dynamic pressure ($q = \frac{1}{2}\rho U_0^2$, where ρ is the air density and U_0 is the mean free-stream velocity). Mathematically, we can write

$$V = Kq\alpha \quad \text{for} \quad -4° < \alpha < 4°, \tag{1}$$

where K is a calibration constant which is 0·165 mV/(deg N m^{-2}) for the yawmeter illustrated. Hysteresis effects are practically nil and the calibration is repeatable within 2 per cent. The small wing size ensures that its lift response is virtually quasi-static up to 12 Hz which is the highest available frequency of oscillatory gusts in this tunnel. The size of the yawmeter does, however, mean that there is some loss of spatial resolution in the x (streamwise) and y (spanwise) directions. The latter is not particularly serious because of the two dimensional (constant with y) nature of the flow being measured.

The dependence of the yawmeter output on dynamic pressure leaves open the question of whether the output is wholly indicative of flow angle. For oscillatory flow, Parker[10] shows that the longitudinal perturbation velocity in the streamwise direction is less than 1 per cent of the freestream velocity for a substantial region around the centre plane of the flow. Thus the yawmeter output can be interpreted as entirely due to flow angle changes because of the small mean velocity variations present in the tunnel.

2.4. Signal Processors

Satisfactory methods for signal processing are a crucial part of any experiment where quantities such as mean values, amplitudes and phase differences need to be derived from unsteady sensor voltage outputs without any adverse effects due to turbulent fluctuations, sensor natural frequencies or electronic noise. In general, any such measurement requires the processing of two sensor outputs; one in a position to supply a reference ('input') condition and the second to record the quantity of interest.

A digital signal processing system is available for oscillatory gust flows at a single frequency. The signal to be measured is sampled digitally at selected instants spread over several oscillation periods. As shown in Fig. 10(i), an input reference signal serves to fix time instant at which a reading of the signal to be measured is taken by a digital voltmeter and recorded by a Hewlett Packard desk top computer. Eight measurements are taken to effectively record one oscillation cycle. The first sample is taken at the beginning of a reference signal oscillation cycle, the second sample at an eighth of a period after the beginning of the next reference cycle and so on till eight readings spaced one and an eighth of a period apart are obtained from eight successive cycles. As shown in Fig. 10(ii), these eight readings can be collapsed together effectively to give all information necessary for knowing one complete cycle. The sampling of successive cycles gives the system enough time to read and record each preceding measurement. The maximum operating frequency is limited by the rate of data transfer to the computer and by the digital voltmeter measurement time of 20 milliseconds. Oscillation frequencies of up to 14 Hz can be handled by the system and this covers the useful frequency range of the gust tunnel. Fig. 11 illustrates a functional box diagram of the system design which is more fully explained in the Appendix. Test measurements show that an average, based on 30 sets of 8 readings, gives results repeatable to a high order of accuracy even with quite high random turbulence fluctuations and electronic noise superimposed on the input signals.

The digital system described above is only reliable for measurements at one frequency. The gust tunnel, however, has been designed to produce a combination of harmonic gusts at two or more frequencies.

To handle the superposition of frequencies, a more generally applicable signal processing system has also been developed. The basic units of the second system are a pair of transient recorders (type DL905) manufactured by Datalab Ltd., each of which have the capability of taking and storing 1000 equally spaced digital samples of a signal using a preselected time interval between each sample. Modifications to the internal clocks of both units enable each of the 1000 samples by both recorders to be taken simultaneously. A step triggering signal, applied to both instruments, starts the sampling sequence at the same instant. The system is operated by using the units to simultaneously record a reference signal (which could be the nozzle motion transducer output or an upstream flow sensor) as well as a response signal from the flow parameter to be studied. The recorded digital data can either be displayed on an oscilloscope for an immediate visual impression or it can be fed into a Hewlett Packard desk top computer for analysis. This machine performs a numerical harmonic analysis of the data to yield the amplitudes at each of the constituent frequencies as well as their phases relative to the corresponding frequency in the input signal. The stored data can also be rapidly plotted by a computer peripheral to give a very detailed view of the waveforms.

The above signal processing system can accurately record other more general types of unsteady flows; the obvious examples being step or ramp gusts as well as periodic, non-harmonic flow variations. In each case, the data analysis can be designed to generate specific information from the available simultaneous digital samples of a reference and measured signal at successive time instants.

Finally, it is to be noted that for qualitative measurements, a wide range of conventional analogue instruments, such as oscilloscopes, filters, r.m.s. meters, etc., are available. Spectral power density measurements are made with a Hewlett Packard analogue spectrum analyser.

3. The Tunnel Flow Characteristics

3.1. Steady Flow

The working section flow characteristics were measured with the nozzle in a stationary, undeflected position. Dynamic pressure measurements were made using a pitot static probe and these indicate no variations with x and y on the horizontal centre plane of the working section. There is a slight increase ($\sim 1{\cdot}5$ per cent) in velocity with vertical distance (z) from the tunnel centreline until the jet mixing regions near the slotted walls are reached. These mixing regions are characterised by a rapid drop in velocity through them. From further measurements, Fig. 12 shows the extent of mixing region encroachment into the central jet flow. The mixing region limits were originally determined without the slotted walls but subsequent measurements, plotted in Fig. 12, show no substantial change due to insertion of the slotted walls. Extensive regions of the jet core exhibit a uniform flow suitable for model mounting over the 2·6 m streamwise length of the working section. Flow angle measurements, within this region of uniform flow, show no measurable variations with x and y although variations with z exhibit a negligibly small (<1 degree) divergence about the centreline of the tunnel flow.

Previous authors (e.g. Parker[10]), working without the slotted walls have shown that the measured steady flow angle induced in the test section is 0·64 of the nozzle angle. The flow angle has been shown to be uniform (with y) across the jet and remains constant with distance downstream. The presence of the slotted walls, however, tends to straighten out the deflected flow; the flow angle aft of about $x = 0{\cdot}80$ m is virtually zero with change in nozzle angle.

3.2. The Unsteady Flow Mechanism

The shear layers above and below the semi-open jet flow in the working section are the primary generators of the unsteady flow. Any movement of the nozzle, oscillatory or otherwise, perturbs these shear layers causing them to roll up into discrete vortices in the mixing regions of the jet. These rolling up vortices convect downstream and induce a travelling wave type of unsteadiness in the jet core. Shear layer perturbations produced by sinusoidal motion of the nozzle plates induce a harmonic oscillatory flow in the working section. Other flow patterns such as non-harmonic periodic and non-periodic gusts are produced by corresponding motions of the nozzle.

The flow structure has been illustrated by two flow visualisation experiments. In the first test, smoke was used in a small scale model of the gust tunnel, complete with a movable nozzle. Plate II shows a photograph of the resulting flow with sinusoidal motion of the nozzle plates. The upper and lower shear layers can be seen to be rolling up into discrete alternating vortices which are convecting downstream. The experiment was at a very low Reynolds number and a high Strouhal number (both based on distance, h, between the movable nozzle plates) compared to the full scale facility.

A second investigation was carried out using a larger model on a water table. Here, the Strouhal numbers of the model and full scale facility were equivalent although the model Reynolds number was small giving a separating laminar boundary layer at the nozzle exit. Streak lines in the flow were visualized by dye and Figs. 13, 14 and 15 show sketches of the flow patterns obtained. Fig. 13 illustrates typical results for oscillatory nozzle motion showing the rapid rolling up of the vortices and their considerable growth as they convect downstream. Fig. 14 displays the corresponding sketches for the nozzle oscillating at a higher frequency in which case the vortex streets tend to remain of the same size as they convect downstream. Fig. 15 illustrates dye streak lines in the flow for a step nozzle input. This case is discussed further in Section 3.5.

Both flow visualisation tests show that a large increase in concentration (due to rolling up) of shear layer vorticity occurs downstream of the nozzle. Thus, large rates of gust amplitude increase with x are a feature of the tunnel flow. The water table experiments did show that slotted walls at certain positions in the mixing regions dissipated the strength of the rolling up vortices as they increased in size. This result was the basis for

incorporating upper and lower slotted walls in the full scale working section to obtain a more uniform distribution of gust amplitude with x. Section 3.3 describes this aspect of tunnel development in more detail.

It is relevant to note that current knowledge of the response to perturbations of laminar shear layers has been reviewed by Michalke[11]. Several detailed experimental investigations of this phenomenon are reported and give an insight into the flow mechanism operating in the gust tunnel. Michalke and Wille[13] excited a plane separated shear layer by harmonic sound pressure fluctuations from a loudspeaker. These fluctuations, by their harmonic nature, produced a shear layer response which was practically identical to that observed in the flow visualisation experiments described above. Browand[14] extended these measurements to the downstream development of the rolling up process. Initially, the shear layer velocity fluctuations, indicative of the rolling up process, increase almost exponentially with downstream distance. At larger distances downstream, the growth of a subharmonic oscillation at half the excitation frequency is apparent. The growth mechanism leading to a subharmonic is of interest since a subharmonic response appeared in initial experiments in the gust tunnel. Theoretically, it can be shown that the initial rapidly rising rolling up process can be described (Betchov and Criminale[15]) by an inviscid, linearised form of the Navier Stokes equations with suitable assumptions for the nearly parallel flow under consideration. It appears that the subharmonic derives from the nonlinear terms which become significant as the excited disturbances in the shear layer increase. Kelly[16] has shown theoretically that the nonlinear terms in the governing equations give rise to a subharmonic but only after the amplitude of the fundamental disturbance has grown to a critical value. Kelly also shows that this subharmonic will eventually dominate the resultant oscillation further downstream. Physically, it appears that once the rolling up vortices from the fundamental disturbance reach a certain size, adjacent vortices tend to slip round each other by mutual induction and eventually fuse into a single larger vortex. It is this fusion of adjacent vortices which induces a subharmonic oscillation in the surrounding flow. A striking illustration of this is given by the flow visualisation picture in Plate III obtained by Freymuth[12]. The experimental work of Browand also shows that these subharmonic fluctuations tend to be of an intermittent nature and the overall flow development remains closely two dimensional up to large distances downstream. Both of these properties have also been observed in the gust tunnel flow.

3.3. Oscillatory Harmonic Gusts at Discrete Frequencies

Up to the present time, research work with the facility has concentrated mainly on tunnel calibration and testing with oscillatory harmonic flows. In the early development stages, spectral analysis tests were undertaken. These revealed that for low frequencies, the flow response was at the forcing frequency. For increasing frequencies and downstream positions, however, the flow responded more and more at half the nozzle forcing frequency. Fig. 16(i) illustrates the spectral results of data from a hot wire probe placed at $x = 1{\cdot}32$ m. For a relatively high forcing frequency of 25 Hz, the flow response was predominantly at the half frequency, 12·5 Hz. Further tests showed that this half frequency could be almost completely suppressed by fitting vortex generators to the inside surfaces of the upper and lower flexible extensions at points 0·38 m ahead of the nozzle lips. The predominant response was then at the forcing frequency (Fig. 16(ii)). Spectra of flow response as measured by a hot wire for various frequencies have shown that with vortex generators, the oscillation energy is concentrated in a band centred on the forcing frequency. A very small half frequency is still discernible.

Tests without the vortex generators have shown that the separating boundary layer at the nozzle exit is laminar even at the highest tunnel velocities. This is due to relaminarisation which must have occurred in the high favourable pressure gradients present on the inside walls of the contraction with its large area ratio. The introduction of the vortex generators, however, provokes transition so that the boundary layer at the nozzle exit is turbulent. From the mechanism of subharmonic formation described in Section 3.2, it appears that the mutual induction and fusion of adjacent vortices in the shear layer is much more likely for the laminar shear layer with its attendant small thickness. The thicker separating shear flow with the vortex generators appears to delay or even prevent subharmonic growth. Experiments with the gust tunnel have shown that the occurrence of subharmonic fluctuations can be intermittent and this agrees with observations by Browand and others (*see* Section 3.2). Theoretically, subharmonic growth can only start after the primary rolling up wave has reached a certain critical amplitude; which ties in with gust tunnel observations that the highest subharmonic amplitudes appeared at high nozzle perturbation amplitudes and at larger distances downstream of the nozzle. It is felt that the form of the separating velocity profile at the nozzle exit plays a significant part in the flow development and the possibility of subsequent subharmonic growth.

The gust tunnel flow characteristics described below are those with the slotted walls inserted in the upper and lower shear layers. These walls serve to damp down excessive growth of the rolling up vortices in the

downstream half of the working section and as such only affect the downstream variation of gust amplitude significantly. Flow variations with frequency and nozzle amplitude in both transverse directions are not unduly affected. It is to be noted that these slotted walls, being a recent innovation, were not utilised in previous work (refs. 10 and 17 to 22).

Fig. 17 shows a typical flow response to oscillatory perturbations at various frequencies. The r.m.s. gust angle, ε_{grms}, at $x = 1{\cdot}300$ m is plotted against frequency parameter (ω/U_0 in m^{-1}) for a freestream velocity of 20·00 m/s at various perturbation amplitudes. These amplitudes, E_{rms} in volts, are expressed in terms of the nozzle displacement transducer output for convenience. A peak response from the flow is obtained at about 8 Hz with fall offs on both sides. For the oscillatory flow, a Strouhal number, fh/U_0, can be defined based on distance h between the movable nozzle plates. From the frequency response at different freestream velocities, a Strouhal number at peak response of roughly 0·35 is obtained. It is probable that basing the Strouhal number on a characteristic shear layer length scale at separation from the nozzle would provide a more precise representation of the frequency of peak response at different freestream velocities in terms of a Strouhal number. Similar response curves with frequency have been obtained by other workers (Freymuth[12], Michalke[11]) in the experimental and theoretical study of excited free laminar shear layers.

Fig. 18 shows typical curves of gust amplitude against x for a range of frequencies at $U_0 = 20{\cdot}00$ m/s. The constant amplitude region aft of $x = 1{\cdot}0$ m is apparent at all frequencies and is a direct result of inserting the slotted walls at optimum positions in the working section (Fig. 3). Without the slotted walls, the gust amplitudes exhibit almost exponential increases in magnitude with downstream distance x.

Typical variations of gust angle amplitudes with vertical distance along the z axis are given in Fig. 19. A 'hyperbolic cosine' type of variation is obtained and it is consistent with the existence of alternating vortices in the upper and lower shear layers. Changes in the variation of ε_{grms} against z with frequency come out of simple theoretical predictions since separation distances between adjacent vortices in each shear layer are frequency dependent. The 'hyperbolic cosine' type of vertical distribution imposes a considerable restriction on the height of uniform amplitude region available for model mounting in the working section flow. If ±5 per cent is taken as the maximum acceptable amplitude variation with z, then for a high frequency parameter of $\omega/U_0 = 5{\cdot}06$ m^{-1}, there is only an 11 cm high region suitable for model mounting around the working section centre plane. However, for an intermediate frequency ($\omega/U_0 = 3{\cdot}03$), this region extends to 15 cm and increases up to 40 cm for the low frequency parameter of $\omega/U_0 = 1{\cdot}01$.

Fig. 20 displays curves of gust amplitude, ε_{grms}, against nozzle amplitude (expressed as E_{rms}) at $x = 1{\cdot}300$ m for several frequencies. These curves are linear for small nozzle angles, although significant non-linearities are indicated in the flow mechanism at larger nozzle amplitudes. A set of graphs like the one in Fig. 20 provide the operating calibration curves for the tunnel at a particular freestream velocity and downstream station.

The downstream convection velocity of the shear layer vortex streets gives the gust tunnel flow its travelling wave nature. The wave velocity imparts linear changes of phase lag (relative to upstream flow) with x and measurements of these quantities are plotted in Fig. 21 as phase lag/metre (ϕ_g/x) against frequency parameter/metre (ω/U_0). The gradient gives the relationship:

$$\phi_g = 1{\cdot}64\,\frac{\omega x}{U_0}$$

and a travelling wave convection velocity, Q, of 0·61 U_0. Experiments have shown the wave velocity to be independent of frequency, nozzle perturbation amplitude and downstream distance x.

Measurements of spanwise uniformity across the working section show a closely two dimensional flow with deviations of less than ±3 percent in gust angle amplitude and less than ±2 percent in phase angles. These variations are of the same order as uncertainties in the measurement system.

Fig. 22 displays envelopes of possible amplitude-frequency combinations at $x = 1{\cdot}300$ m for freestream velocities of 12·43 and 20·00 m/s. Test conditions of constant gust angle amplitude ($\varepsilon_{grms} = 1°$) for a frequency parameter/metre range of $0{\cdot}4 < (\omega/U_0) < 5{\cdot}7$ as well as constant frequency parameter ($\omega/U_0 = 2{\cdot}5$) for an amplitude range of $0° < \varepsilon_{grms} < 2{\cdot}7°$ are available in the facility. Although both frequency and amplitude ranges are somewhat limited, the flow oscillations are harmonic throughout this range. Photographs of two oscilloscope traces of typical outputs from the gust tunnel are shown in Fig. 23. The upper traces are of the nozzle displacement transducer output which is proportional to instantaneous nozzle angle from the horizontal while the lower traces are of the instantaneous gust angle variation measured by the aerofoil yawmeter at $x = 1{\cdot}300$ m on the tunnel centreline. The superimposed high frequency oscillation at about 200 Hz in these traces is the resonance frequency of the aerofoil yawmeter structure.

Mathematically, the oscillatory vertical gusts available on the flow field centreline can be given by the equation

$$\varepsilon_g(x, t) = \varepsilon_{gpk}(x)\, e^{i\omega[t-(x/Q)]}, \tag{3}$$

where ω is a radian frequency, Q is a travelling wave velocity equal to 0·61 of the freestream velocity, U_0, ε_g is an instantaneous flow angle and ε_{gpk}, the peak amplitude of flow angle, is a function of frequency, downstream distance, x and the nozzle perturbation amplitude as illustrated in the preceding calibrations (Figs. 17, 18 and 20).

A fundamental change in the flow field of the gust tunnel can be obtained by placing a horizontal splitter plate in the centre plane of the working section, as shown in Fig. 24. The oscillatory flow just above the splitter plate is now induced by a series of vortices in the upper mixing region together with a series of effective image vortices in the lower mixing region and vice versa for the flow just below the splitter plate. The induced flow oscillations near the plate in the jet core are now streamwise of the form

$$U(x, t) = U_0 + U_1(x)\, e^{i\omega[t-(x/Q)]}, \tag{4}$$

where ω is the radian frequency, U is the instantaneous velocity, U_0 is the constant mean freestream velocity, Q is the convection velocity of the travelling wave and U_1, the amplitude of velocity oscillations is a function of frequency, downstream distance, x, and nozzle perturbation amplitude. Tunnel characteristics for this 'U-oscillation' mode are virtually identical in form to the calibrations described earlier for the 'gust' mode except that the r.m.s. gust angle, ε_{grms}, is replaced by a nondimensionalised r.m.s. amplitude of streamwise velocity, U_{1rms}/U_0. Static pressures on the splitter plate in oscillatory flow have also been measured and yield results consistent with the velocity variations above the plate. The only major difference between the 'U-oscillation' and 'gust' modes of tunnel operation is in the value of the travelling wave convection velocity. Measurements of phase lag/metre (ϕ_u/x) against ω/U_0 for the 'U-oscillation' mode give the relationship

$$\phi_u = 1{\cdot}29\frac{\omega x}{U_0}, \tag{5}$$

shown plotted in Fig. 21. A travelling wave velocity of 0·77 U_0 is obtained as compared to 0·61 U_0 for the 'gust' mode. It is believed that the difference in wave velocity between the two modes arises from the mutual induction of vortices and their image systems in the upper and lower shear layers.

3.4. Oscillatory Harmonic Gusts at Combinations of Two Frequencies

Flow conditions in the gust tunnel have been extended to include combinations of gusts at two frequencies. The electro-hydraulic actuator system produces displacements of the nozzle frame which follow an input voltage signal made up of the sum of two discrete frequencies. The perturbed shear layers on the edges of the flow respond by rolling up into a system of vortices which induce gusts in the working section at the two forcing frequencies.

The results of a qualitative spectrum analysis showed that the flow responded at the two input frequencies only. No discernible traces of subharmonics or higher harmonics were detected. Furthermore, no response peaks were observed at frequencies which were a sum or difference of the two constituent frequencies making up the nozzle input. These results were encouraging with respect to the well defined frequency content of the gust response available in the tunnel. Fig. 25 displays a detailed frequency response at two freestream velocities. The response is expressed in terms of the gust angle amplitude per unit amplitude of nozzle displacement ($\varepsilon_{gpk}/E_{rms}$). The representation is permissible, since the variation of ε_{gpk} with E_{rms} is approximately linear and yields a graphical representation which takes the nozzle amplitude into account. A particular pair of identical points in Fig. 25 plot the flow response at a dual frequency input which is made up of the two frequencies given by the abscissae of the points. The oscillatory responses for single frequency inputs are also shown as full lines for comparison.

It is observed from Fig. 25 that available amplitudes for double frequency inputs are significantly reduced in comparison to the single frequency response. These results cannot be a basis for any general conclusions because they were obtained by restricting nozzle input combinations to those with zero phase difference between the two frequencies. It will be shown subsequently that a change in the phase difference does alter the amplitudes of the two frequencies in the flow response. In overall terms, the frequency range for which usably

large amplitudes are available has the same limitations as in excitation at a single frequency. A peak response is obtained at a Strouhal number of approximately 0·35 together with a usable frequency range of 2 to 10 Hz at $U_0 = 12{\cdot}43$ m/s and 4 to 12 Hz at $U_0 = 20{\cdot}00$ m/s. Thus, nozzle excitation with $U_0 = 12{\cdot}43$ m/s at a combination of 8 Hz and 16 Hz will yield a flow response at 8 Hz only with virtually no amplitude at 16 Hz. In spite of this limitation, a wide range of frequency parameters (in m^{-1}) are still available ($0{\cdot}63 < \omega/U_0 < 6{\cdot}3$).

Gust amplitude variations with x in this mode of tunnel operation were measured for a range of input conditions and Fig. 26 illustrates typical results for $U_0 = 20{\cdot}00$ m/s. The amplitudes at both frequencies level out to fairly uniform amplitudes aft of $x = 1{\cdot}00$ m. Furthermore, plots of phase change with downstream position against x for each frequency result in linear relationships from which the phase change per metre (ϕ_g/x) can be derived for both the frequencies. Typical values of ϕ_g/x are plotted against ω/U_0 in Fig. 21 and show that the relationship of equation (2) holds for each frequency of the nozzle input signal. An unchanged travelling wave velocity of $0{\cdot}61\ U_0$ is obtained. Response measurements with double frequency inputs have only been made for the 'gust' mode of the tunnel.

Typical amplitude variations with z for each of the constituent frequencies are shown in Fig. 27. Similar results for other frequency combinations also display the 'hyperbolic cosine' type variations which were observed for oscillatory flow at single frequencies. This similarity also applies to amplitude and phase measurements in the y direction which reveal an oscillatory flow with very good spanwise uniformity.

Finally, some measurements have been made to oberve changes in flow response due to a phase difference between the two frequencies comprising the input. Here the phase difference with respect to the period of the higher frequency component is relevant since a relative shift between the two frequencies along the time axis equal to one period of the high frequency component will encompass all possible waveforms that any phase shift between the two frequencies could produce. Fig. 28 illustrates the results with variations of gust angle ampliitude per unit nozzle amplitude against phase difference. The large variations obtained here are more than ten times the error estimates of the data recording system and show an ordered amplitude variation with phase difference for both frequency components. There is considerable uncertainty about the development and structure of the rolled-up vortices in the shear layers under excitation at a combination of two frequencies. This rolling-up structure must alter in significant ways due to phase change between the two frequencies and thus accounts for the above observations. At the moment, it is sufficient to have a gust tunnel facility which can produce well known oscillatory flows at a combination of two frequencies.

3.5. Tunnel Response to Step Nozzle Inputs.

Parker[10] did some preliminary work to bring out tunnel flow response for step inputs without using the slotted walls. Fig. 29 illustrates typical results for a downward step input of the nozzle plates. Initially, the flow response is in the opposite direction to that of the main gust as shown by portion B to C of the response curves. At C, the flow angle starts to move rapidly back in the main gust direction and eventually overshoots to a peak at D after which this 'transient' approaches the final steady flow angle asymptotically at E. The result of a flow visualisation experiment with a step nozzle input (Section 3.2) is shown in Fig. 15. The inward (towards the flow) motion of one of the nozzle plates during the step induces a large rolling up vortex in its corresponding shear layer. The existence of this vortex (which grows as it convects downstream) between the start and end of the step change ties in with the flow response exhibited in Fig. 29. The magnitudes of the peaks at C and D increase with downstream distance which would be expected from a rolling up and growing vortex convection downstream. This growth in size would also cause a spreading out of the response with time as the gust convected downstream and this is also evident in Fig. 29. The flow visualisation results do show some rolling up of the upper shear layer corresponding to the nozzle moving away from the main flow although this is small compared to the rolling up in the lower shear layer. The nozzle rise time for the step is 72 ms while the flow response time from the initial undisturbed state to the final flow angle varies from 0·17 s for $x = 0{\cdot}61$ m up to 0.21 s for $x = 1{\cdot}219$ m.

These results show that sharp edged step gusts in the flow are precluded by the tendency of the bounding shear layers to roll-up during nozzle motion. Adequate sharp edged gusts could probably be produced by a detailed shaping of the nozzle motion with time between the initial and final positions so as to incorporate controlled under or overshoots. Parker's preliminary work is capable of some extension in this area.

4. Experimental Investigation

The gust tunnel's unsteady flow capabilities have been utilised in several research programmes. These fall into two broad categories—the first consisting of research into aspects of fundamental fluid mechanics

(Pocha[17], Wasserson[18] and Patel[19,20]) and the second on aircraft aerodynamic response to unsteady flows (Parker[10], Hancock[21] and Taylor[22].

Wasserson and Pocha investigated the effects of oscillatory gusts on the flow around two-dimensional circular and square cylinders respectively. The relationships between response effects at the natural shedding ('Strouhal') frequency and the forcing frequency in the flow were a principal result of these investigations. At flow frequencies near the Strouhal frequency, most of the energy in the flow fluctuations was observed to be at the flow frequency. At this stage, the flow frequency is said to have 'captured' the Strouhal frequency so that the vortex shedding occurs at the flow frequency. This result was apparent for both square and circular cylinders together with evidence of strong interference between periodicity in the potential flow and the periodicity of the vortex shedding phenomenon over the test frequency range.

Patel used the tunnel in its 'U-oscillation' mode to obtain experimental data on laminar and turbulent boundary layer response to streamwise velocity oscillations of a travelling wave character (equation (4)). His results showed that oscillating pressure gradients produced by the travelling wave character of the freestream had a dominant effect on the response of both laminar and turbulent layers although these were significantly affected by the frequency of oscillation. For the laminar boundary layer, the experimental data showed good agreement with a theory developed to apply in regions of low and high frequencies. A mathematical model of the turbulent boundary under the influence of high frequency oscillations was also developed using a modified eddy viscosity concept to account for turbulence. Although agreement with experiment was poor in this case, the theory highlighted physical aspects of turbulent boundary layer response to an oscillating freestream. This investigation was restricted to boundary layers under a zero mean pressure gradient. Work is now under way in the Aeronautical Department to extend these results and theories to cases involving mean pressure gradients as well as to look at the effect of an oscillating freestream on separation of a turbulent boundary layer.

Work on aircraft aerodynamic response to oscillatory gust flows was started off by Parker with experimental data for a delta wing with chamfered non-symmetrical leading edges in cross-section. The effects of this leading edge asymmetry on lift, pitching moment and surface pressures in both steady and oscillatory flows were quite significant. Comparisons between the experimental data and linearised theories for oscillatory flow yielded fairly good agreement. Considerable qualitative information has also been presented for the delta wing response to the 'saw-tooth' type of gusts obtained in the tunnel with step nozzle inputs (*see* Section 3.5).

Hancock describes a model suspension rig for the gust tunnel by which the dynamic response of a complete aircraft model to unsteady flows in heave and pitch was investigated. Measurements of unsteady aerodynamic derivatives enabled an estimated dynamic response to be calculated. Comparisons with the measured dynamic response showed reasonable agreement for heave amplitudes although pitch amplitudes were completely underestimated by the calculations. Comparisons between phase angle results were inconclusive because of measuring inaccuracies caused by the lack of adequate data processing equipment at the time. Some measurements of transient response behaviour of the model in its suspension rig were also made using the 'saw tooth' gust described in Section 3.5. Comparison of this response with a theoretical estimate showed surprisingly good agreement. This work underscores the potential of developing free flight rigs which enable the dynamic response characteristics of a complete model aircraft to be measured in the gust tunnel facility.

More recently, Sylvia Taylor has made measurements of rolling moment and side force in oscillatory sideslip flows for a series of swept wing-fuselage models. The effects of incidence, mean sideslip angle, dihedral and wing height on the fuselage were investigated in these experiments. A vortex lattice theory was developed to calculate rolling moments due to both oscillatory and steady sideslips. The results showed good overall agreement with the experiments.

A current research programme is aimed at measuring the forces (lift and pitching moment) on wing planforms in oscillatory gust flows. A selection of simple planforms with streamwise tips and varying aspect ratio, sweep and taper are being tested together with two delta wings of aspect ratios 1 and 2. Detailed force measurements have also been made on a wing planform immersed in oscillatory flow at a combination of two frequencies, to verify the principle of superposition.

5. Conclusions

In oscillatory flow, gust angle fluctuations in the working section are strongly sinusoidal so that the bulk of the flow energy is concentrated within a narrow band centred on the frequency of nozzle motion. Fig. 22 illustrates an 'envelope' curve of the available amplitude-frequency combinations. Maximum amplitudes are available at frequencies corresponding to a Strouhal number (fh/U_0) of approximately 0·35. These amp-

litudes fall off at frequencies on either side of this region, and result in a situation where the usable frequency range decreases as the required flow amplitude increases. In spite of this, large frequency and amplitude ranges are available. Typically, for a freestream velocity of 20·00 m/s, these test conditions consist of a frequency range of 3 Hz to 13 Hz at a constant gust angle amplitude ($\varepsilon_{grms} = 1°$) as well as an amplitude range of $0 < \varepsilon_{grms} < 2{\cdot}70$ at a constant frequency (8 Hz).

Fig. 18 illustrates a typical spatial variation of amplitude with x in the working section. A constant amplitude region is obtained aft of $x = 1{\cdot}00$ m up to the end of the working section at $x = 2{\cdot}600$ m. The 'hyperbolic cosine' type variation of gust amplitude with vertical distance z restricts the height of the uniform amplitude region available for model mounting in the flow, particularly at high frequencies. Measurements of spanwise (with y) variations of gust amplitude and phase reveal a closely two dimensional flow field.

The travelling wave character of the oscillatory flow is caused by the downstream convection of the rolling up vortex streets in the shear layers. Measurements yield a constant wave velocity (Q) of 0·61 U_0 for all frequency and amplitude conditions. Mathematically, the flow can be expressed as

$$\varepsilon_g(x, t) = \varepsilon_{gpk}(e)\, e^{i\omega[t-(x/Q)]}, \tag{3}$$

where $Q = 0{\cdot}61\ U_0$. It must be noted that this value of travelling wave velocity applies only for the 'gust' mode of tunnel operation. The facility can be operated in a 'U-oscillation' mode by the insertion of a splitter plate in the horizontal centre plane of the nozzle and working section. The frequency response and spatial distributions of the streamwise velocity amplitude is unchanged from the flow angle variations for the 'gust' mode. The only major change is in the value of the travelling wave velocity for these streamwise velocity oscillations. The form of oscillation is

$$U(x, t) = U_0 + U_1(x)\, e^{i\omega[t-(x/Q)]}, \tag{4}$$

where $Q = 0{\cdot}77\ U_0$; remaining constant over the tunnel operating conditions.

Oscillatory flows at combinations of two frequencies provide a useful addition to the test conditions available in the gust tunnel. The flow response under excitation with two frequencies is such that either component frequency is amplified according to its position in the discrete frequency response curve. Thus, for example, a component frequency at the peak of the tunnel response is amplified greater than another frequency near the fringes of the discrete frequency response. Moreover, a component frequency which is not within the tunnel response is not amplified at all so that the resulting flow has very little energy at that forcing frequency. Measurements of flow response amplitude at each of the two component frequencies do show that the 'double' frequency response cannot be built up by superposition from the well known discrete frequency response. Amplitudes of both component frequencies are also altered significantly by relative phase change between the frequencies making up the excitation. The failure of superposition to apply is a consequence of the nonlinear nature of the rolling up mechanism generating the oscillatory flow. Its only effect on the facility as an experimental tool is that every flow situation required in the working section has to be individually calibrated for.

The spatial amplitude variations of the component frequencies closely follow results already described for discrete frequency excitation. Thus, all the comments made there apply for the amplitudes of component frequencies in this mode. Figs. 26 and 27 show typical results which carry forward to the definition of a region of acceptably uniform amplitude, displayed in Fig. 12. These results demonstrate that the unsteady flow facility possesses a considerable potential for development in the generation of gusts at combinations of several frequencies. The possibility of producing gusts with a known and adjustable spectral power density has wide implications for wind tunnel tests in unsteady flows which are more representative of reality.

The generation of non-periodic gusts requires the removal of the slotted walls due to their attendant flow straightening effects. The preliminary work done in this area (Section 3.5) is capable of considerable development.

The unsteady flow facility provides a useful research tool capable of generating a variety of flow conditions for testing purposes. In oscillatory flow there are limitations on the available frequencies and amplitudes as well as on the volume of the working section flow which is suitable for model mounting. Low tunnel flow speeds together with the necessity for using small models creates problems in the realistic representation of full scale Reynolds numbers. Finally, it must be emphasised that, for unsteady flows, the quality of experimental results obtained from the facility will largely reflect the sophistication of the data reduction equipment employed. It is felt that the tunnel together with its associated digital and analogue instruments provides a complete and effective system for the measurement of unsteady flow phenomena.

Acknowledgments

The authors wish to express their appreciation of the many research workers, technicians and staff of the Aeronautical department who have contributed to the development of the gust tunnel over the last decade.

In particular, the support and technical expertise of Dr. L. G. Whitehead is gratefully acknowledged as having been invaluable to the success of the efforts reported here.

LIST OF SYMBOLS

x, y, z	Fixed cartesian coordinate axes system (*see* Fig. 3(i))
t	Time dimension
E_{rms}	r.m.s. amplitude of oscillatory output from nozzle displacement transducer
f	Frequency in Hz
h	Distance between flexible nozzle plates
K	Aerofoil yawmeter calibration constant
Q	Travelling wave convection velocity
q	Dynamic pressure
r_1 to $r_8(r_n)$	Voltage outputs of single frequency digital method
r, r_0, r_1	Instantaneous, mean and amplitude of oscillatory measured signal respectively
r_r, r_i	In-phase and out-of-phase amplitudes of measured signal respectively
t_0, t_1	Time periods
U_0	Mean freestream velocity
U_1	Amplitude of streamwise velocity oscillations
U_{1rms}	r.m.s. amplitude of streamwise velocity oscillations
V	Yawmeter output voltage
α	Angle of incidence
ε_g	Instantaneous gust angle
ε_{gpk}	Amplitude of gust angle oscillations
$\varepsilon_{\text{grms}}$	r.m.s. amplitude of gust angle oscillations
θ_n	Angles $\frac{\pi}{4}(n-1)$ for $n = 1$ to 8
ρ	Air density
ϕ_g	Phase difference in gust angle oscillations
ϕ_u	Phase difference in streamwise velocity oscillations
ω	Radian frequency ($=2\pi f$)

REFERENCES

No.	Author(s)	Title, etc.
1	C. F. Reid and C. G. Wrestler	An investigation of a device to oscillate a wind tunnel airstream. NASA TN D-739, 1961.
2	J. Gilman and R. M. Bennett	A wind tunnel technique for measuring frequency response functions for gust load analysis. Presented at the Structural Dynamics Session of an Aircraft Design & Technology Meeting, Los Angeles, 1965.
3	J. D. Schetzer	Gust generation experiments. Univ. of Michigan Rept.; NATO AGARD papers presented 16 June–16 July, 1954.
4	R. A. Sawyer	0·7 m×1 m low speed gust tunnel. Dept. of Mech. Eng., Univ. of Salford, England, 1970.
5	K. Hirosue, K. Kitamura, Y. Murakami and S. Shindo	Design and development of the gust wind tunnel at the National Aerospace Laboratory. NAL TR-335, 1973.
6	J. Bicknell and A. G. Parker	A wind tunnel stream oscillation apparatus. *Journal of Aircraft*, Vol. 9, pp. 446–447, 1972.
7	G. K. Hunt, D. R. Roberts and D. Walker	Measurements of transient pressures on a narrow delta wing due to an upward gust. A.R.C. C.P. No. 624, 1961.
8	J. H. Horlock	An unsteady flow wind tunnel. *Aero Quart.*, Vol. 25, pp. 81–90, 1976.
9	B. Satyanarayana, J. P. Gostelow and R. E. Henderson	A comparison between experimental and theoretical fluctuating lift on cascades at low frequency parameters. 19th ASME Int. Gas Turbine Conf., Zurich. Preprint No. 74-GT-78, 1974.
10	A. G. Parker	On delta wings in unsteady flow. Ph.D. Thesis, Univ. of London, 1970.
11	A. Michalke	The instability of free shear layers. Progr. in Aerosp. Sc., Vol. 12, pp. 213–240, 1972.
12	P. Freymuth	On transition in a separated laminar boundary layer. *J. Fluid Mech.*, Vol. 25, pp. 683–704, 1966.

No.	Author(s)	Title, etc.
13	A. Michalke and R. Wille	Strömungsvorgänge im laminar-turbulenten Übergangsbereich von Freistrahlgrenzschichten. Applied Mech., Proc. 11th Intern. Congr. of Appl. Mech. Munich, 1964, pp. 962–972. Ed. H. Gortler, Berlin: Springer, 1966.
14	F. K. Browand	An experimental investigation of the instability of an incompressible separated shear layer. *J. Fluid Mech.*, Vol. 26, pp. 281–307, 1966.
15	R. Betchov and W. O. Criminale	*Stability of Parallel Flows.* New York—London: Academic Press, 1967.
16	R. E. Kelly	On the stability of an inviscid shear layer which is periodic in space and time. *J. Fluid Mech.*, Vol. 27, pp. 657–689, 1967.
17	J. J. Pocha	On unsteady flow past cylinders of square cross-section. Ph.D. Thesis, Univ. of London, 1971.
18	L. R. Wasserson	On a circular cylinder in oscillatory flow. Ph.D. Thesis, Univ. of London, 1971.
19	M. H. Patel	On laminar boundary layers in oscillatory flow. *Proc. Roy. Soc. Lond.* A 347, pp. 99–123, 1975.
20	M. H. Patel	On turbulent boundary layers in oscillatory flow. *Proc. Roy. Soc. Lond.* A 353, pp. 121–144, 1977.
21	G. J. Hancock	An investigation on aircraft model response to unsteady flows. Ministry of Technology Contract—final report, 1971.
22	S. Taylor	Wing-body combinations in unsteady lateral flows. Ph.D. Thesis, Univ. of London, 1975.
23	M. H. Patel	On unsteady boundary layers. Ph.D. Thesis, Univ. of London, 1974.

APPENDIX

Following on from the remarks made in Section 2.3, a detailed description of the digital signal processing system for single frequencies is given here.

As shown in the functional box diagram of Fig. 11, the reference signal is first passed through a variable gain amplifier and a variable tuning bandpass filter. These are followed by a limiting high gain amplifier which converts the resulting sinusoidal signal into a reference square wave. A coincidence switching circuit now, on receiving a start signal, outputs a voltage pulse at the beginning of the next rising square wave cycle. This is for connecting counter 1 to a store and resetting counter 2 to zero at the beginning of each reference square wave cycle. The output of a high frequency (in kHz ranges) square wave oscillator branches directly to counter 2 and to counter 1 through a 'frequency divide by 8' unit. The contents of counter 1 are fed into a store and display once every cycle at the start signal cue. The contents of the store are continuously compared to those of counter 2 by a coincidence circuit which issues a pulse when the two are identical. This pulse is a read and record command for the digital voltmeter and recording circuit elements. Both counters 1 and 2 are reset to zero at the end of every measured set of 8 readings. The output pulse also feeds a logic circuit through a 'frequency divide by 8' unit. This logic circuit resets and starts the whole unit for recording continuously anything up to 15 complete sets of 8 readings.

The amplifier variable gain control is used to adjust the input reference signal amplitude to 0·15 volts (r.m.s.) at monitor plug A on the instrument console. The reference signal must have a zero d.c. bias. The read and record units of the system have been commercially bought. A Solartron digital voltmeter (LM 1420.2) reads the voltage value and feeds it to a Solartron-Schlumberger Data Transfer Unit which serves a Hewlett Packard 9800 Series desk computer. For the record, the Data Transfer Unit consists of a power supply (3238), a manual data input unit (3209), an interface (3205) and an output driver (3221). Some changes have been made to this equipment. The digital voltmeter has now had its polarity switch bypassed so that measurement time for one reading is brought down to 20 milliseconds. Only negatively biased voltages can thus be read but this is no hindrance. Further, the 20 millisecond measurement time serves to average out any mains interference in the signal.

The simple harmonic analysis used in data processing by the computer is outlined below. The eight readings in a cycle are averaged for a measurement over 30 cycles. If $r_1, \ldots, r_n, \ldots, r_8$ are these averaged values, then the analysis gives mean value

$$r_0 = \tfrac{1}{8} \sum_{n=1}^{8} r_n,$$

in phase component

$$r_r = \tfrac{1}{4} \sum_{n=1}^{8} r_n \cos \theta_n,$$

out of phase component

$$r_i = \tfrac{1}{4} \sum_{n=1}^{8} r_n \sin \theta_n,$$

amplitude $= \{r_r^2 + r_i^2\} \times \sqrt{2} \times$ r.m.s. amplitude and phase angle (relative to reference signal) $= \tan^{-1}(r_i/r_r)$ where $\theta_n = ((\pi/4)(n-1))$ for $n = 1$ to 8 represents 8 equally spaced intervals starting with $\theta_1 = 0$ in the reference signal cycle.

There are two calibrations of the digital system that need to be performed. Because of a filter in the reference signal path (Fig. 11), errors are introduced in the phase difference measurements between the two signals. These errors can be eliminated by a suitable calibration involving the filter tuning control. The system is set up to read the same reference and measurement signal from an oscillator. A filter tuning control setting giving zero phase difference can be derived for each frequency from the system results. It is also necessary to apply a correction to amplitude results from the system arising from the 20 millisecond measuring time of the digital voltmeter. As shown in Fig. 30, a measurement at time t_0 will involve an averaging of the result over a small measurement time $2t_1$, say. Taking a general harmonic waveform

$$r_0 + r_1 e^{i\omega t}$$

and averaging over a time $2t_1$, gives the integral

$$\frac{1}{2t_1}\int_{t_0-t_1}^{t_0+t_1}(r_0+r_1\,e^{i\omega t})\,dt = r_0+r_1\frac{\sin\omega t_1}{\omega t_1}e^{i\omega t}.$$

Thus, the measured amplitude has to be multiplied by a constant factor of $(\omega t_1/\sin\omega t_1)$ where ω is the radian frequency and $2t_1$ is the measurement time (20 milliseconds, here).

It can also be shown by analysis (Patel[23]) that the digital system is relatively unaffected by the presence of higher harmonics or a half frequency subharmonic of the fundamental operating frequency in the measured signal. Some uncertainty does exist in the band width of the measuring system adjacent to the fundamental frequency. The results are affected in that turbulence and other flow fluctuations within this frequency band will be measured by the system. The band width reduces with increase in the number of cycles over which one measurement is averaged. It is assumed here that errors from this source are negligible for the 30 sets of 8 readings (per cycle) used in all measurements although this aspect of the system warrants more detailed study.

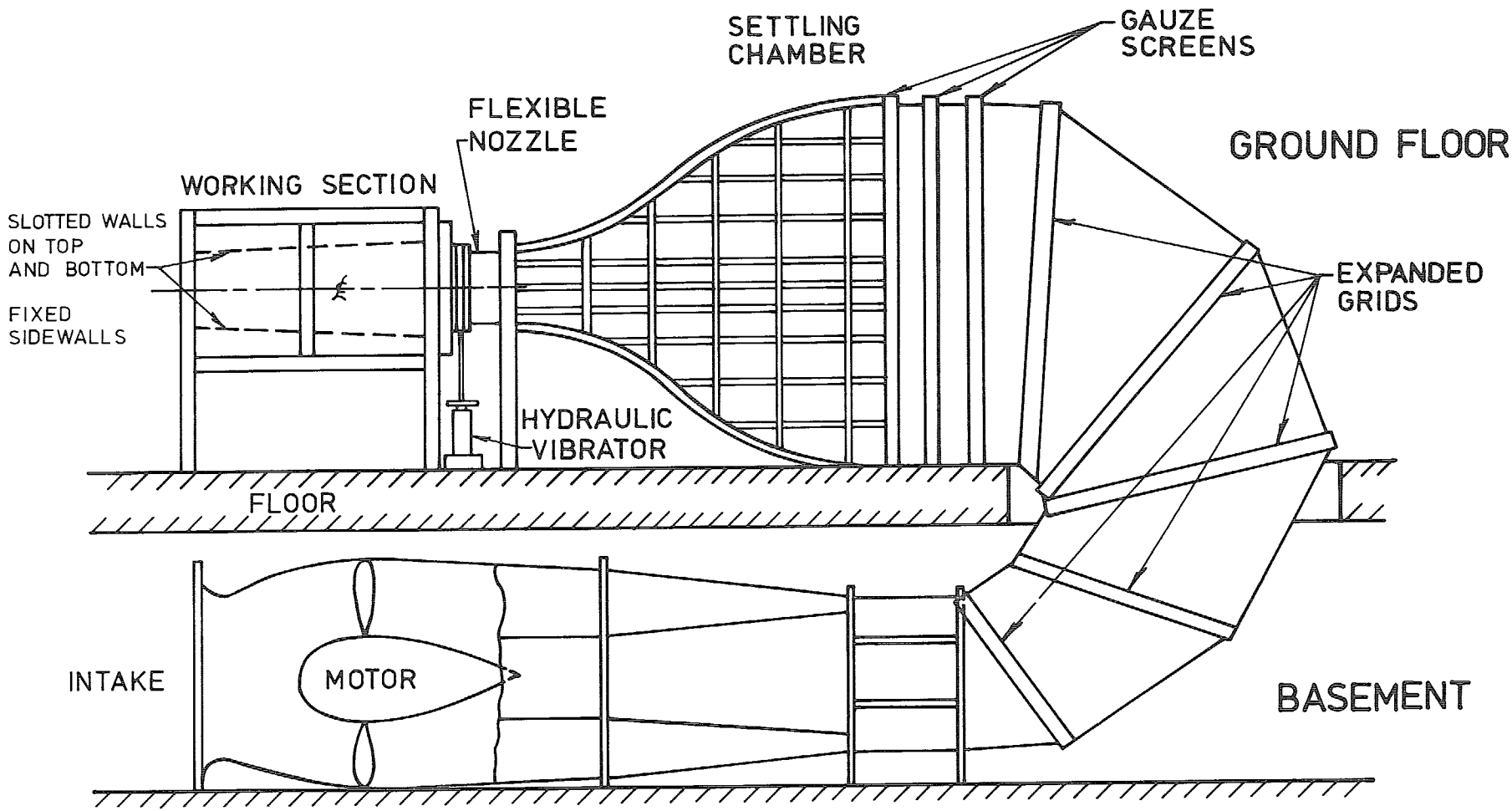

FIG. 1. Unsteady flow facility: the wind tunnel.

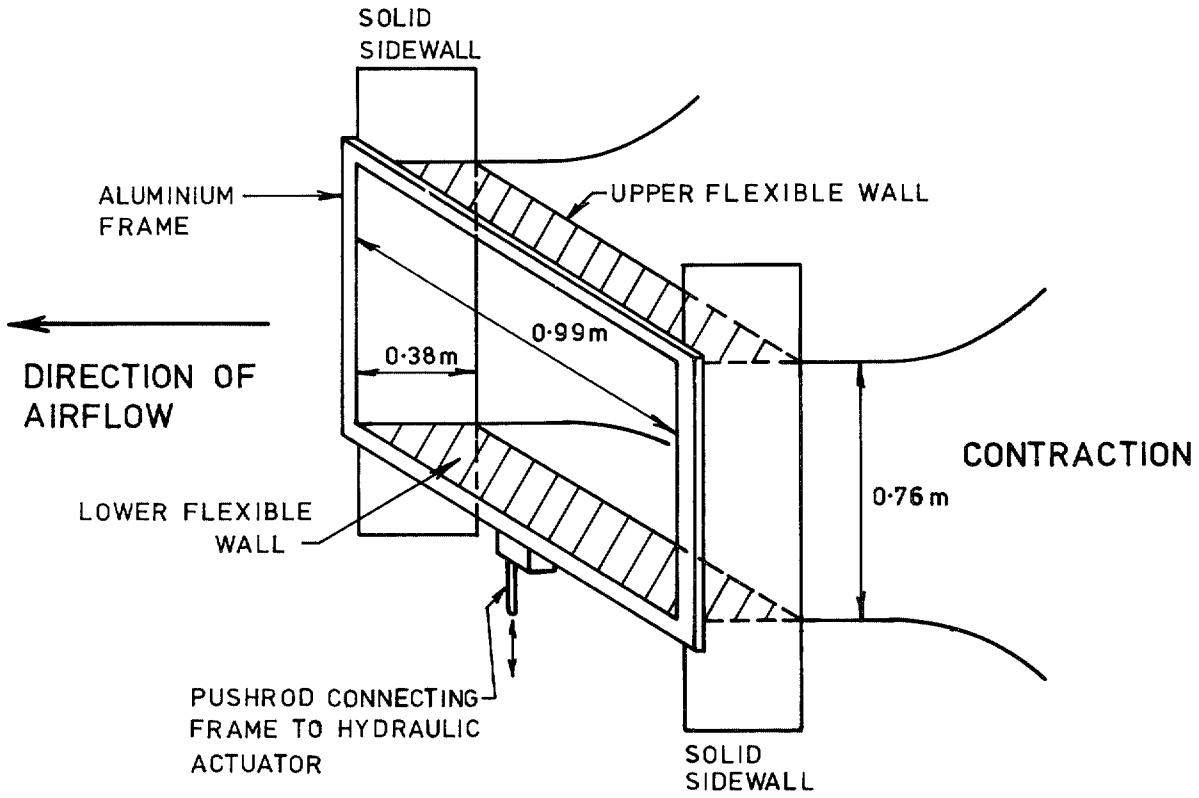

FIG. 2. Flexible nozzle details.

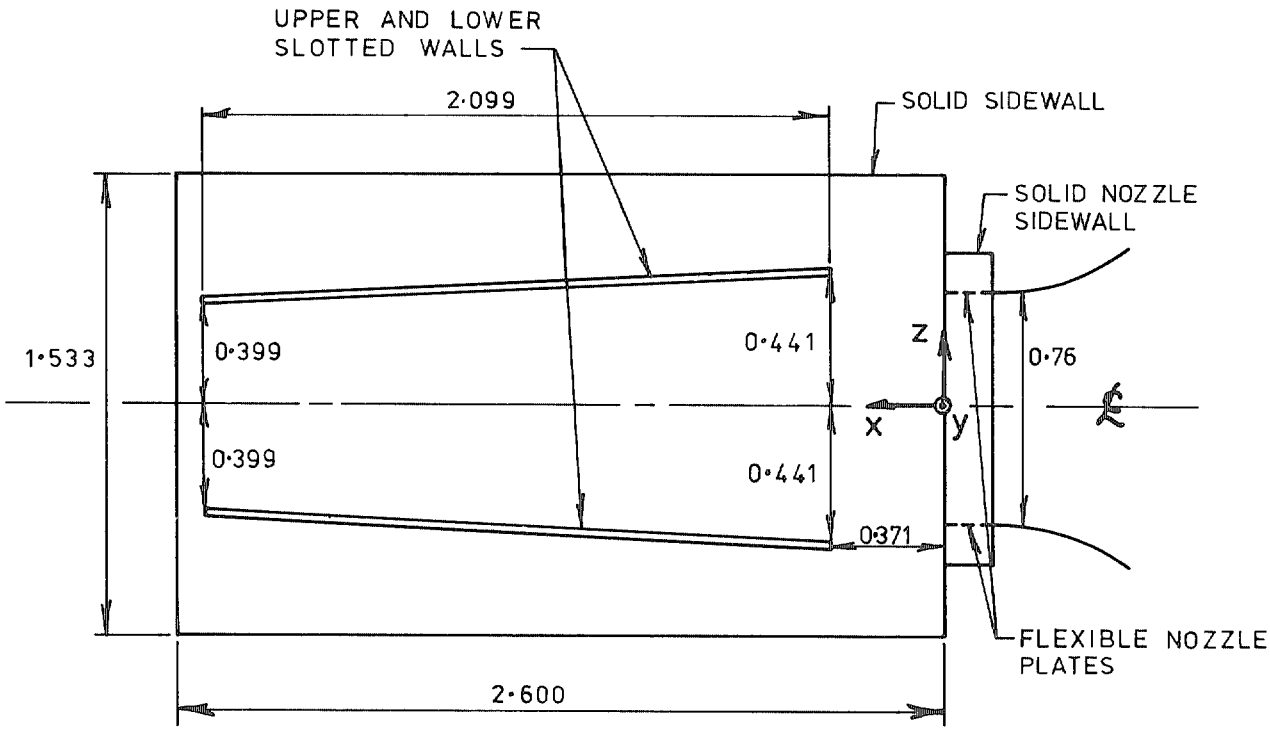

SLOTTED WALL POSITIONS IN WORKING SECTION

Fig. 3(i)

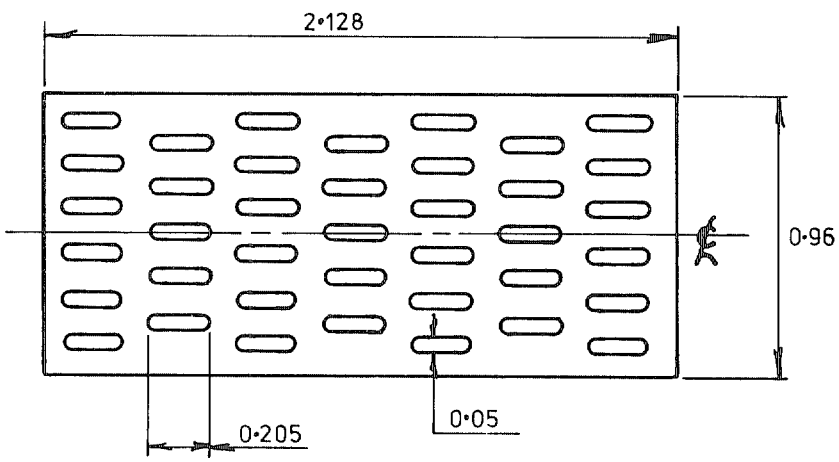

ALL DIMENSIONS IN METRES

SLOTTED WALL PLAN VIEW

Fig 3(ii)

FIG. 3. The slotted walls.

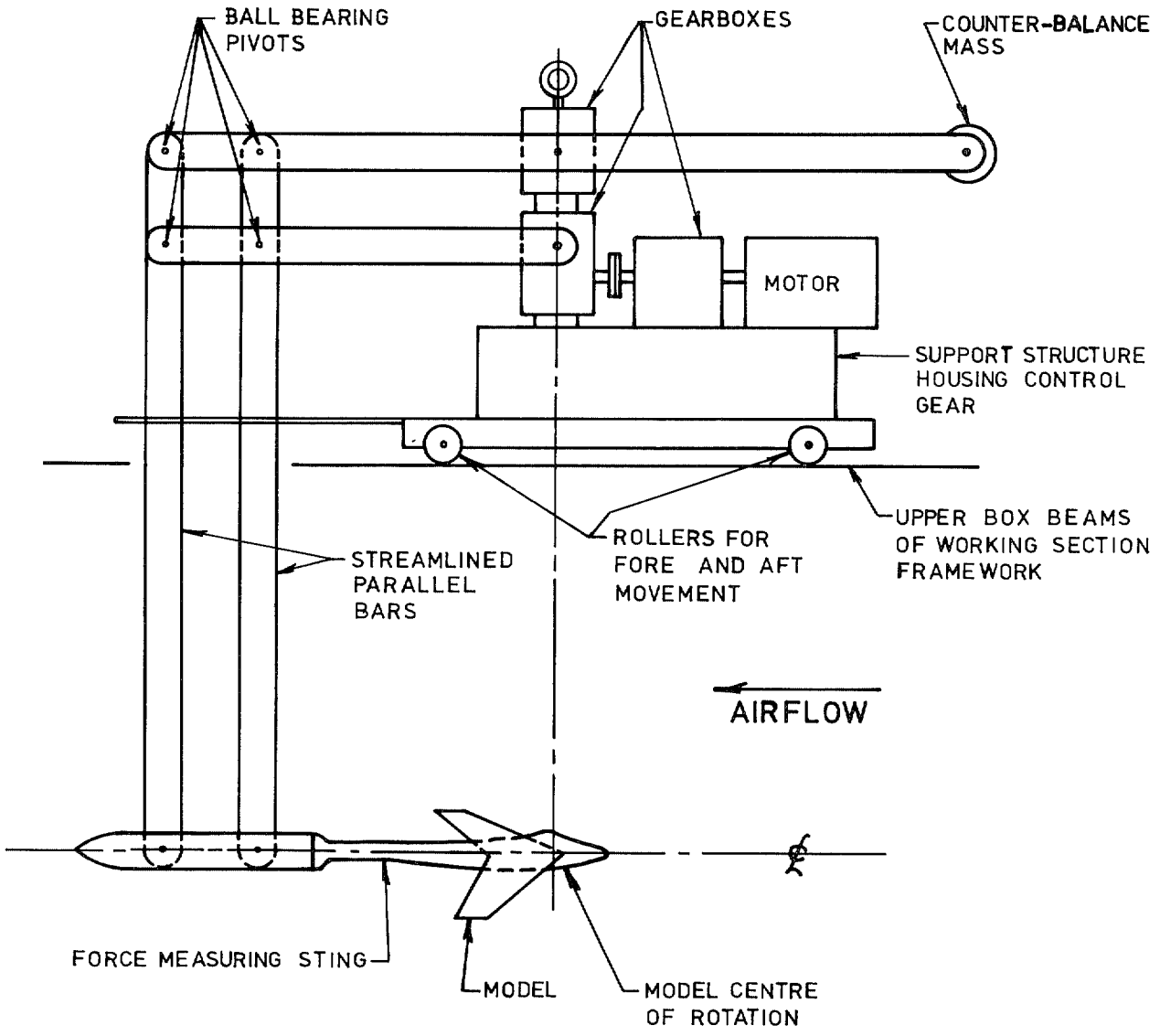

FIG. 4. Model mounting rig.

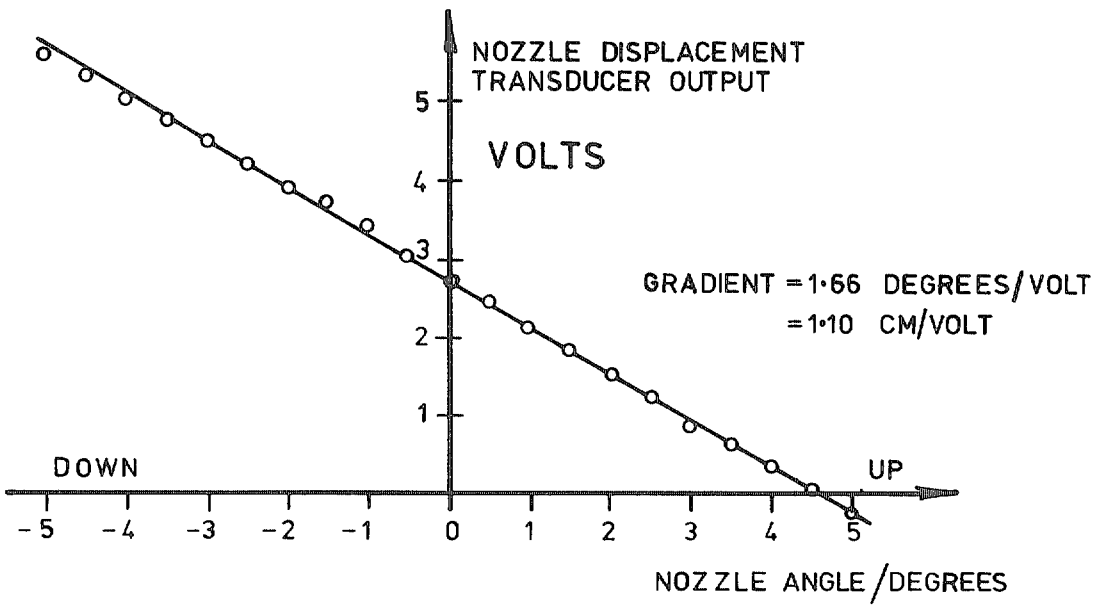

FIG. 5. Nozzle transducer calibration.

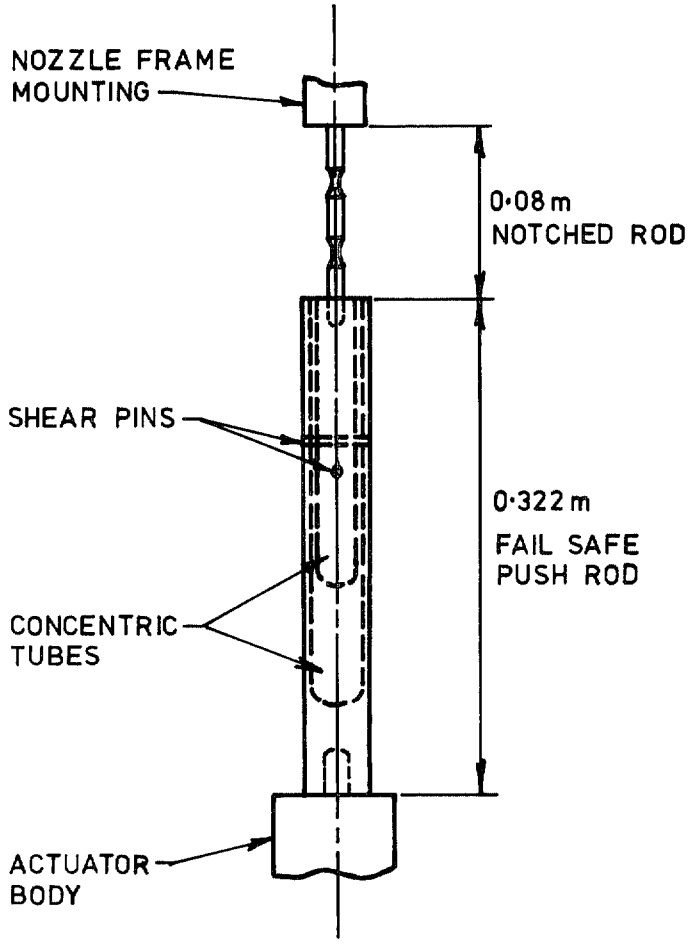

FIG. 6. The nozzle actuator connecting rod.

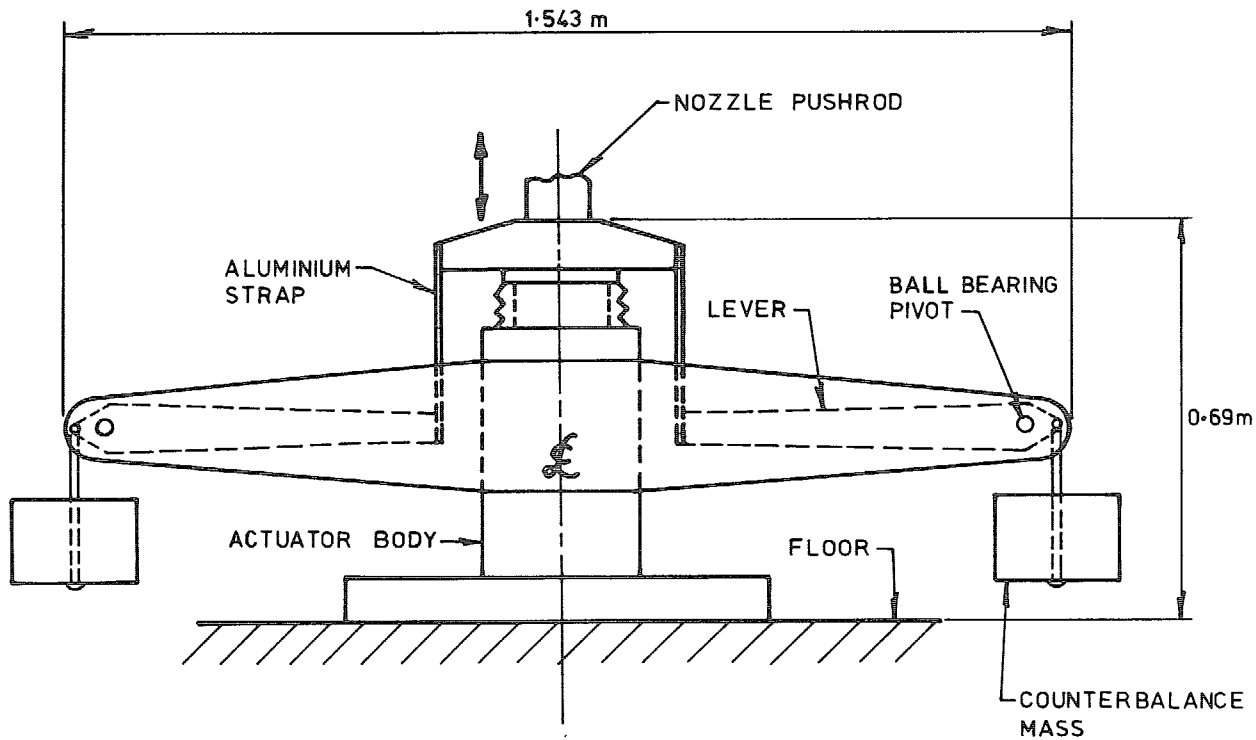

FIG. 7. The nozzle actuator balancing mechanism.

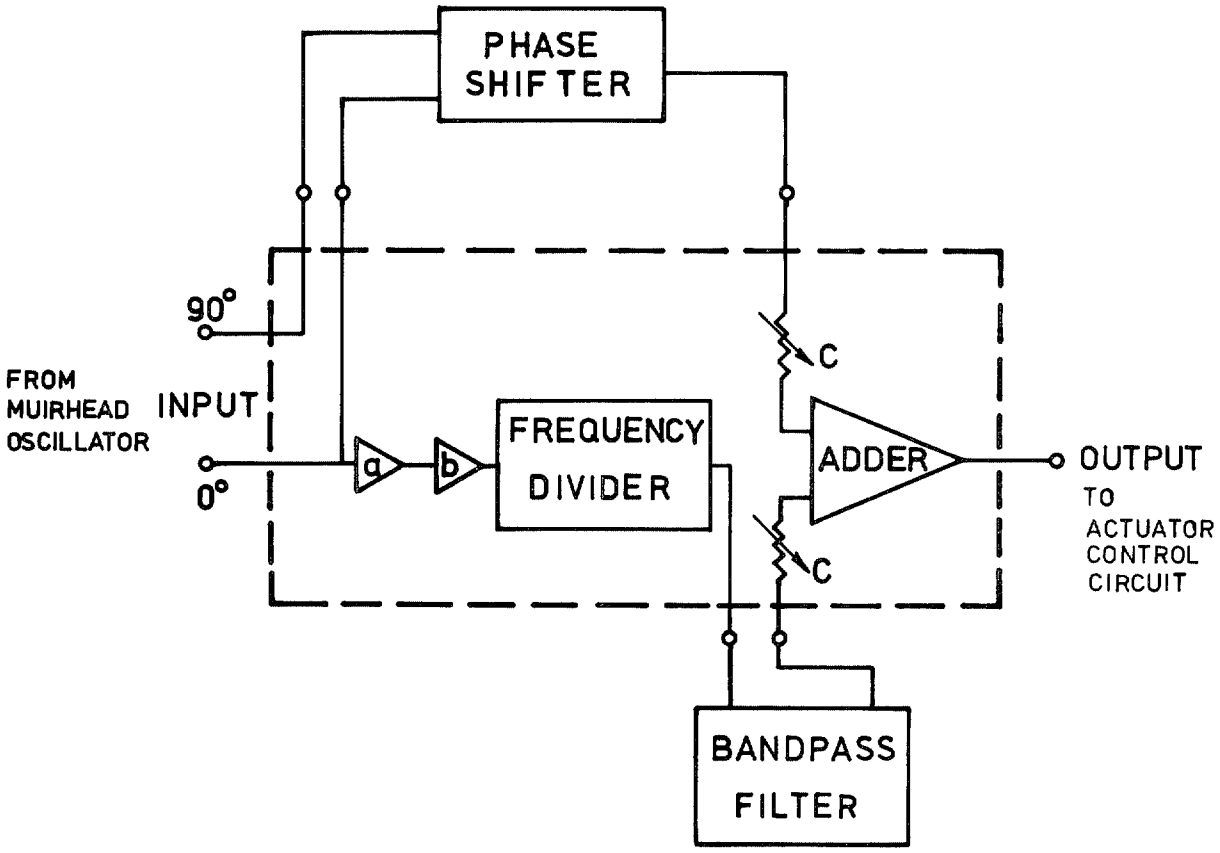

a) - BUFFER AMPLIFIER
b) - LIMITING HIGH GAIN AMPLIFIER
c) - AMPLITUDE SELECT POTENTIOMETERS

FIG. 8. Block diagram of system for producing an oscillatory signal at a combination of two frequencies.

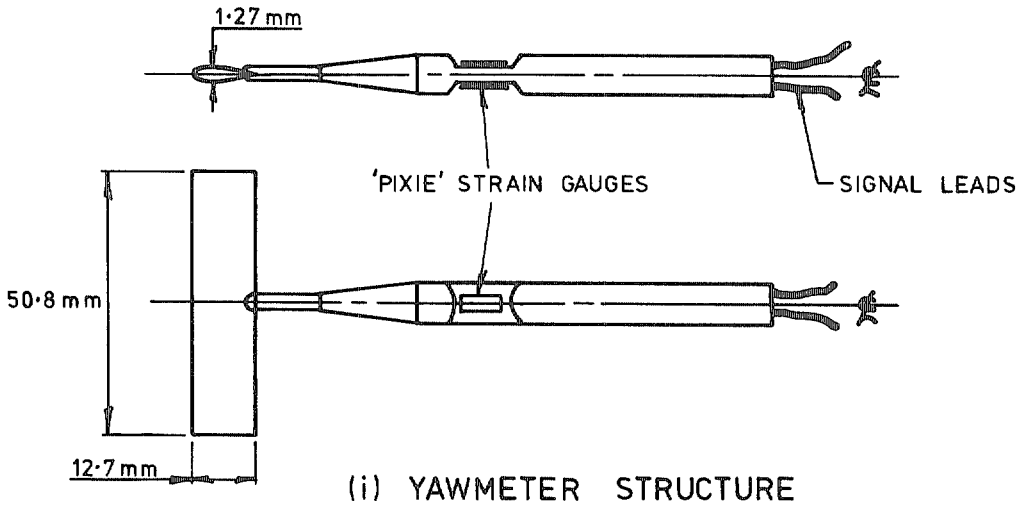

(i) YAWMETER STRUCTURE

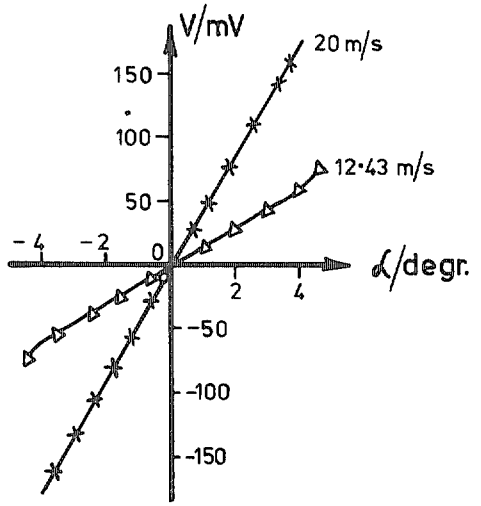

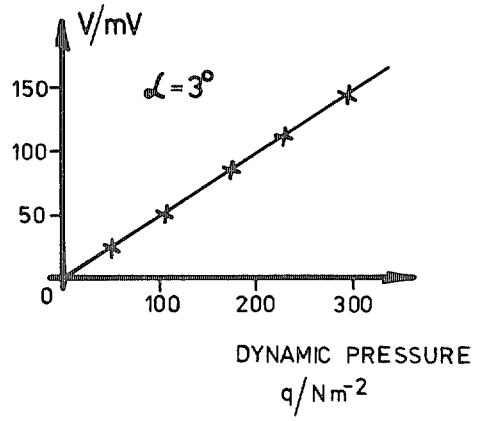

(ii) CALIBRATIONS FOR FLOW ANGLE AND DYNAMIC PRESSURE

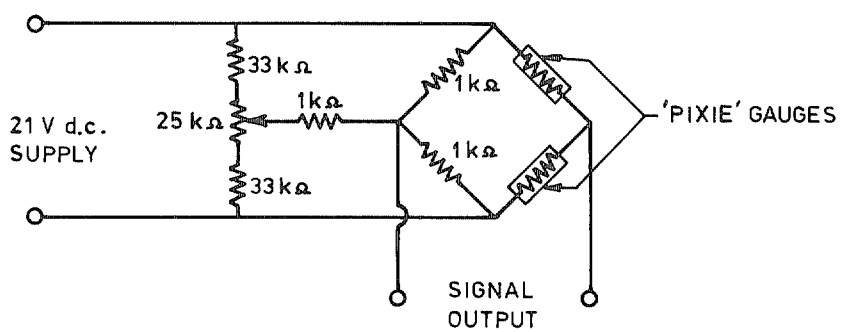

(iii) BRIDGE CIRCUIT

FIG. 9. The aerofoil yawmeter.

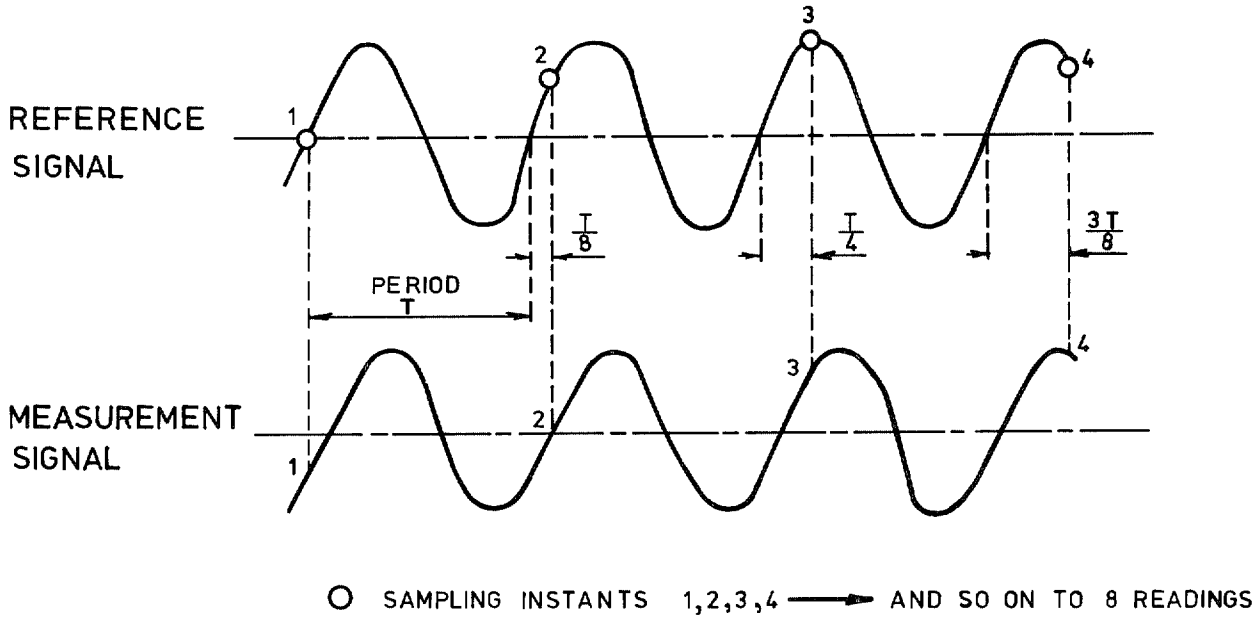

(i) ACTUAL SAMPLING SEQUENCE

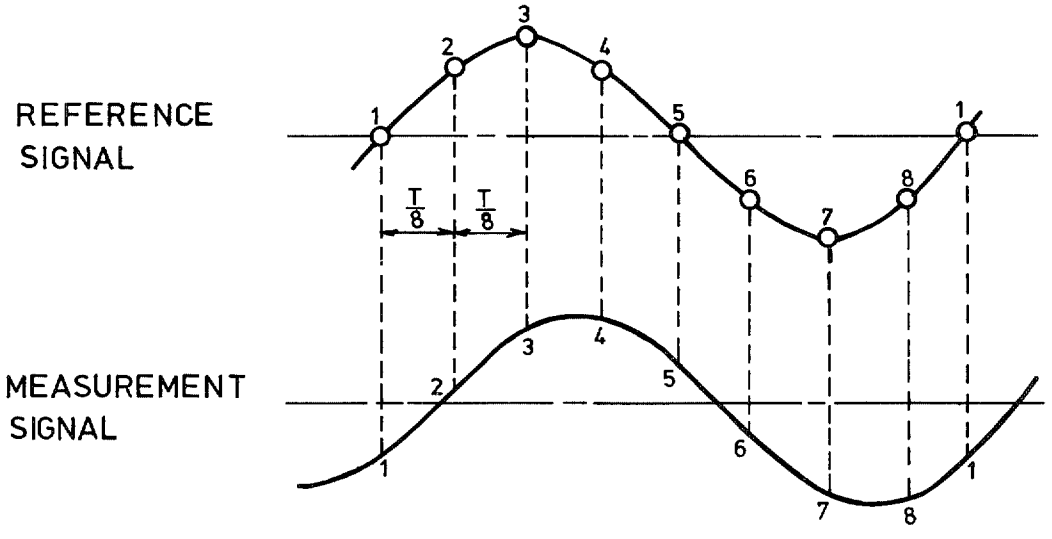

(ii) EFFECTIVE CYCLE SAMPLING

FIG. 10. Sampling sequence.

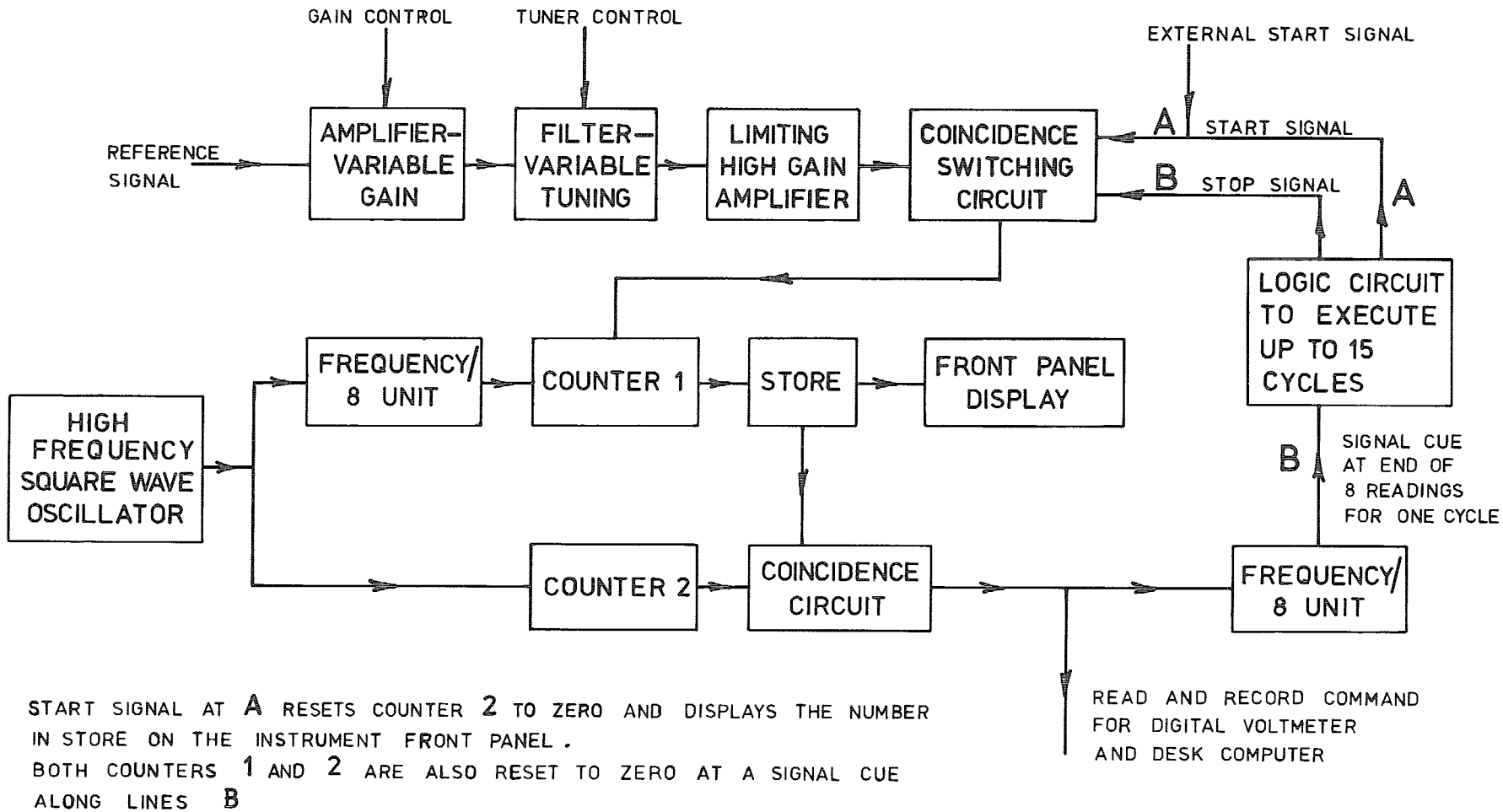

FIG. 11. The digital sampling system for single frequencies.

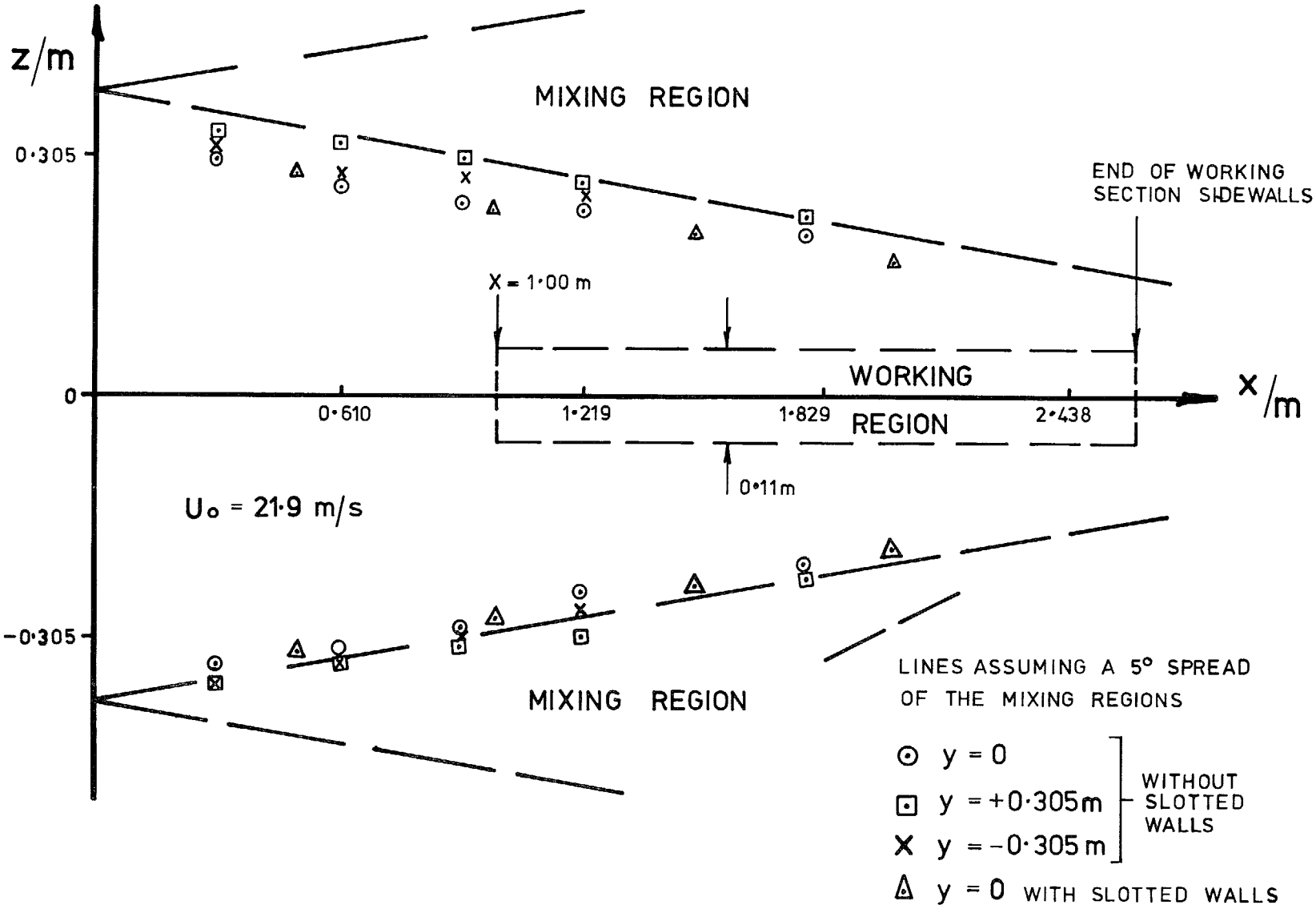

FIG. 12. Mixing region positions.

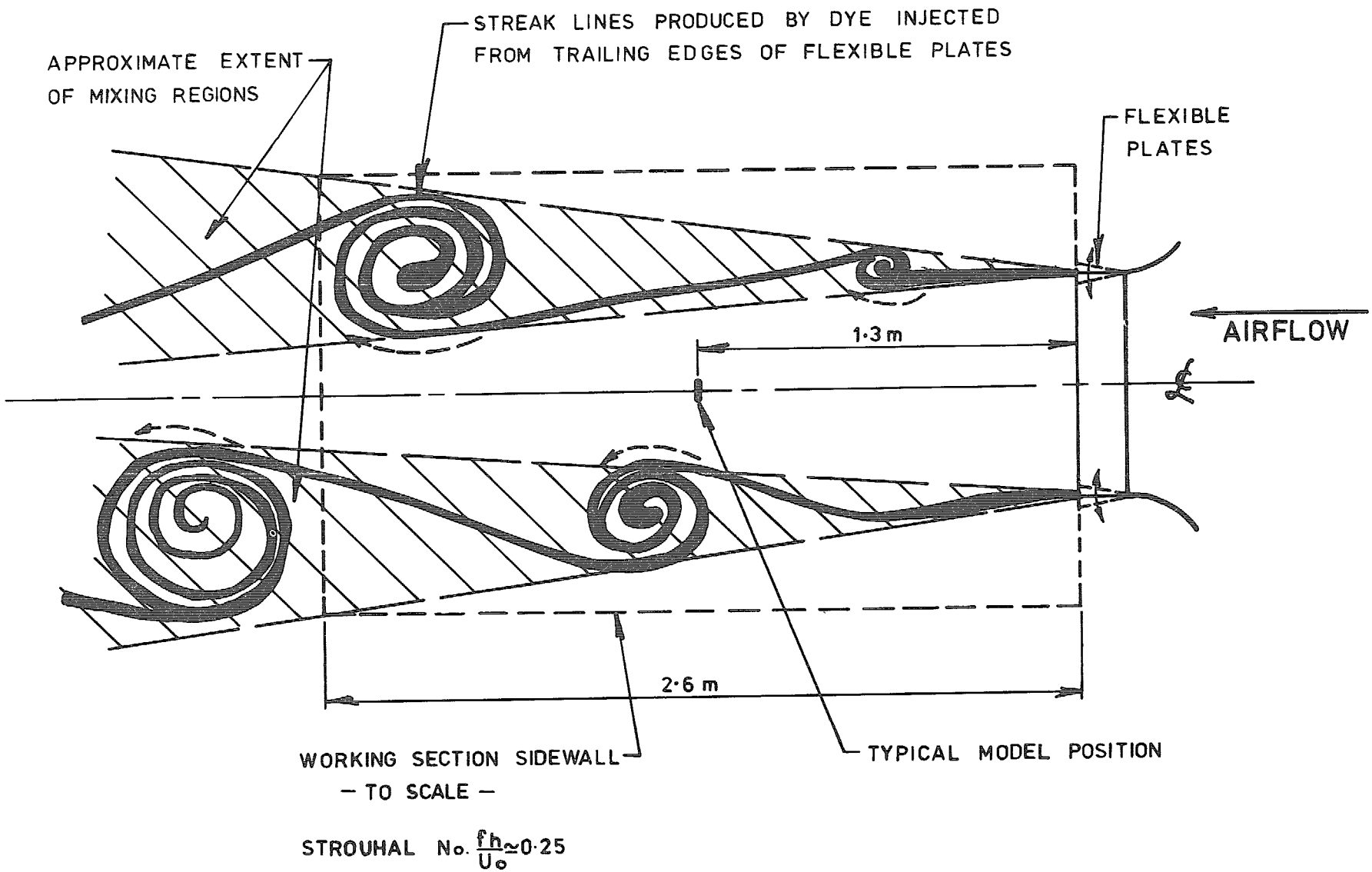

FIG. 13. Sketch of flow field for low frequency nozzle oscillation.

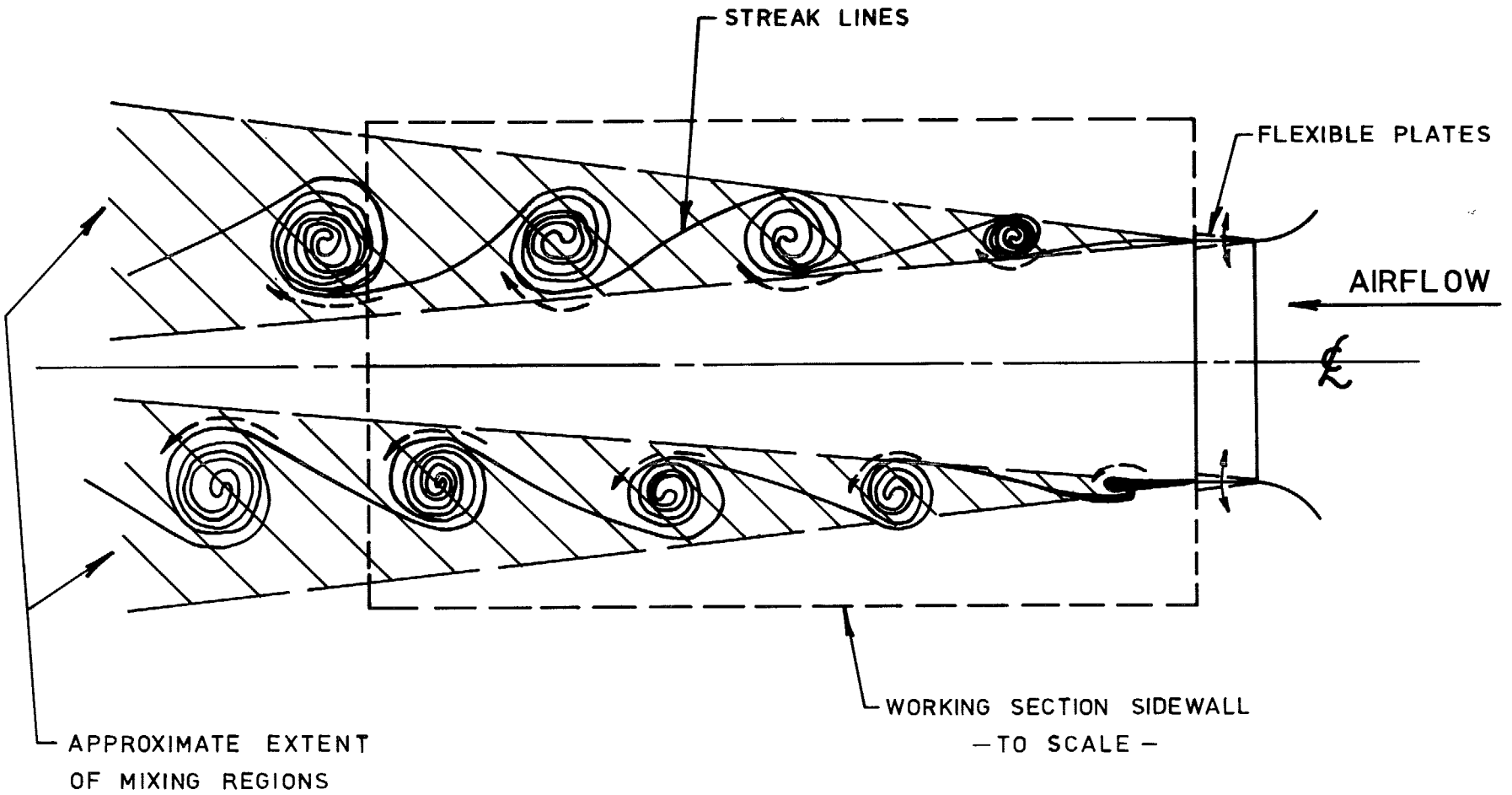

FIG. 14. Sketch of flow field for high frequency nozzle oscillation.

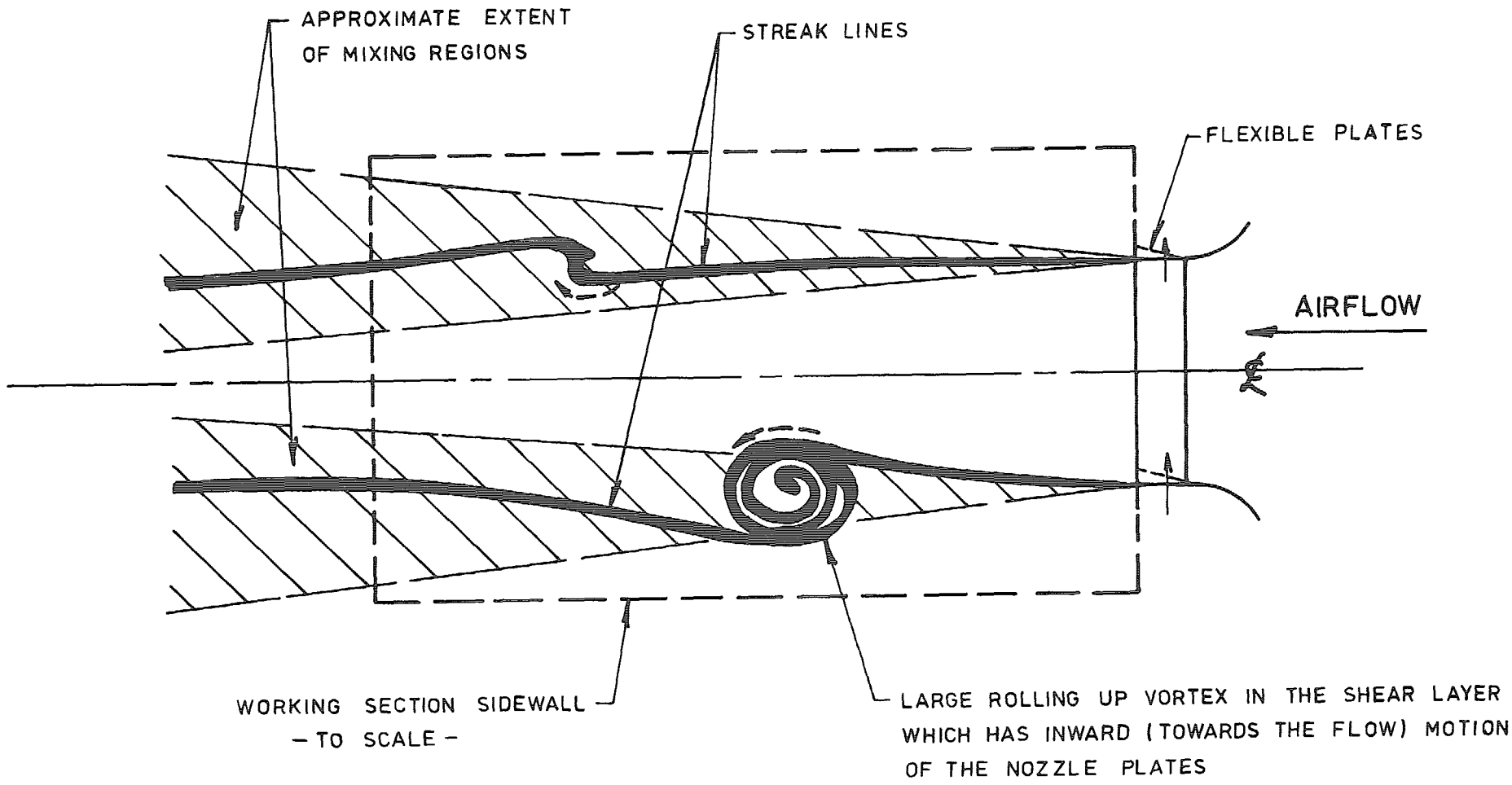

FIG. 15. Sketch of flow field for upward step motion of the nozzle plates.

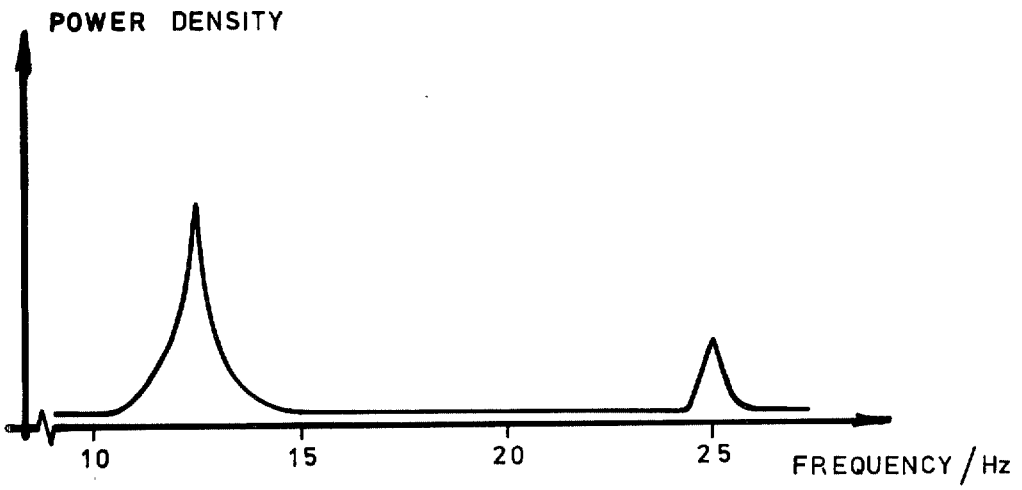

(i) NO VORTEX GENERATORS

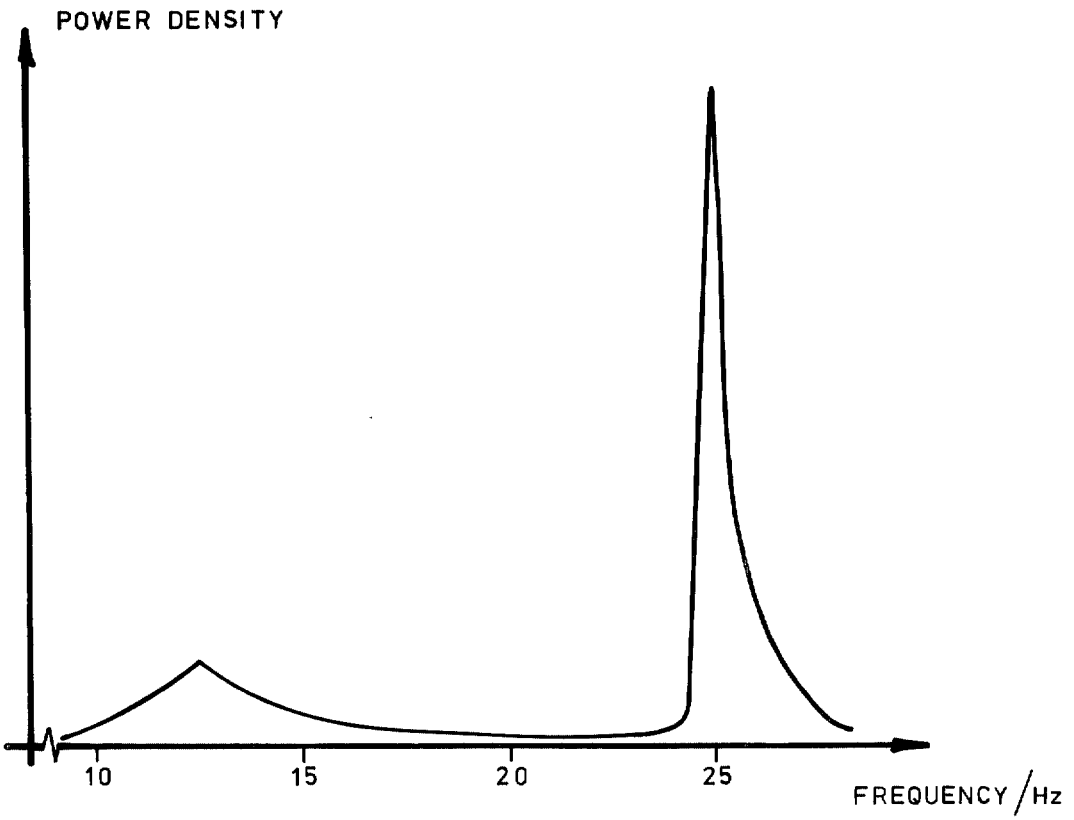

(ii) WITH VORTEX GENERATORS

FORCING FREQUENCY = 25 Hz X=1·32M y=z=0

FIG. 16. Frequency spectra.

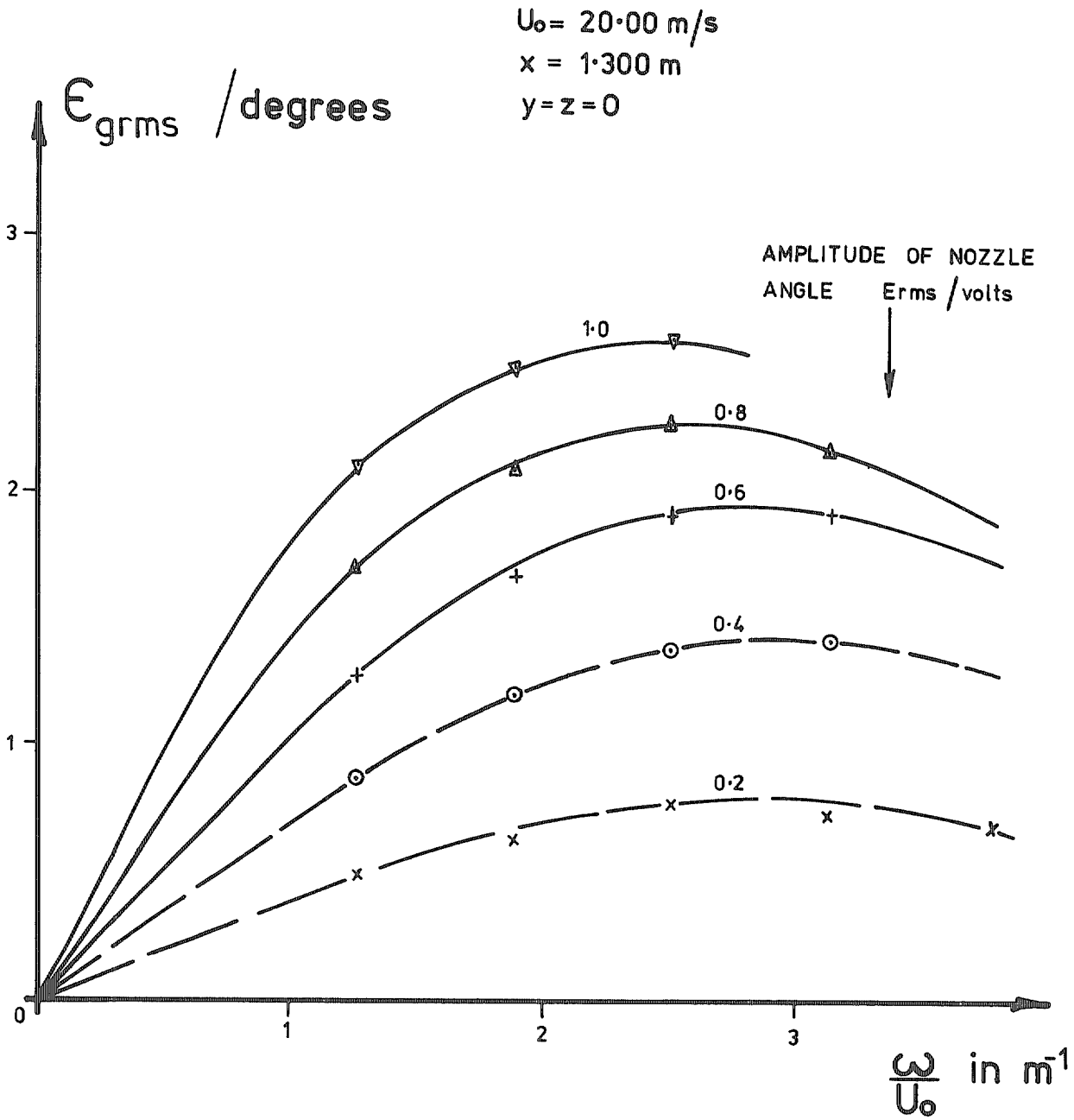

FIG. 17. Gust angle amplitude variation with frequency.

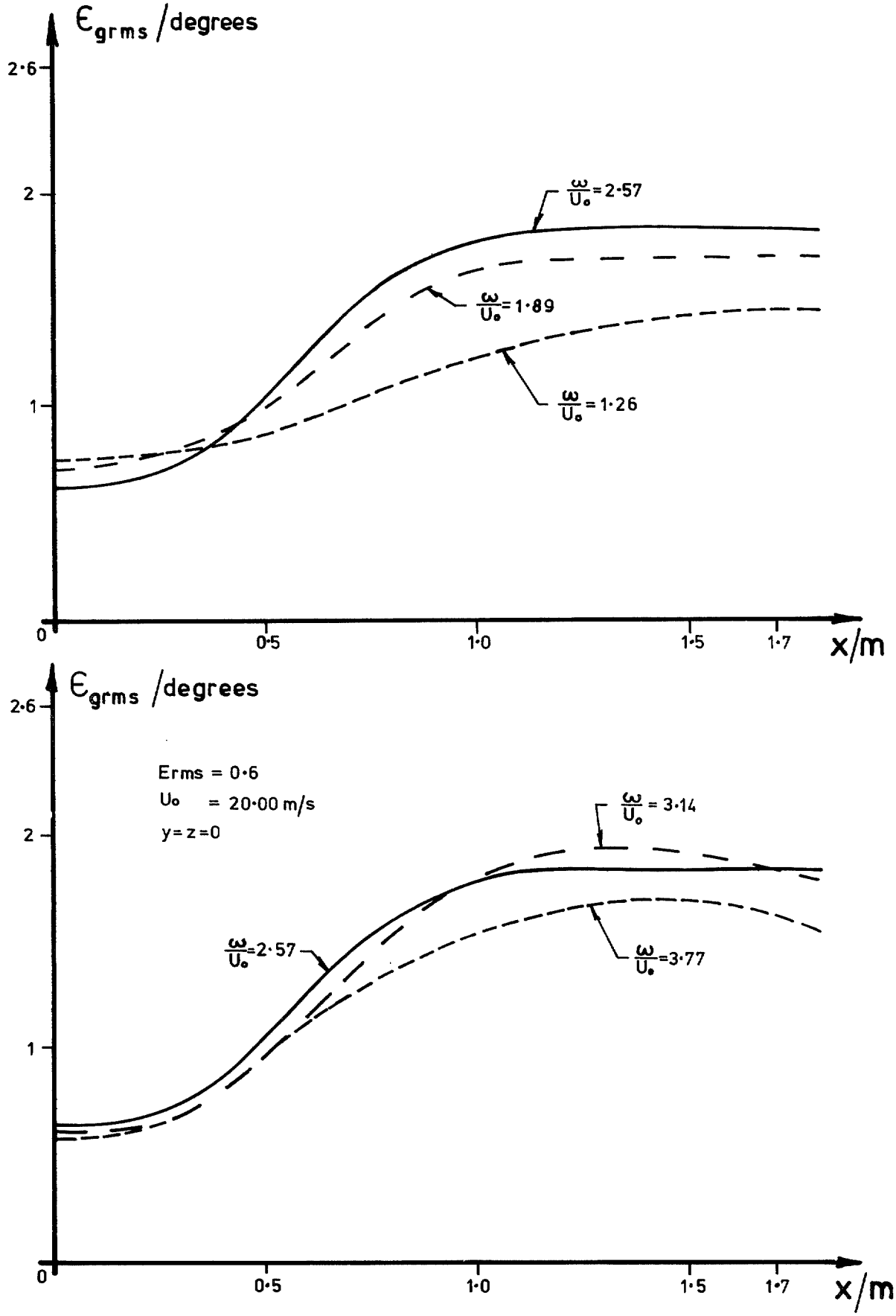

FIG. 18. Gust amplitude variation with x.

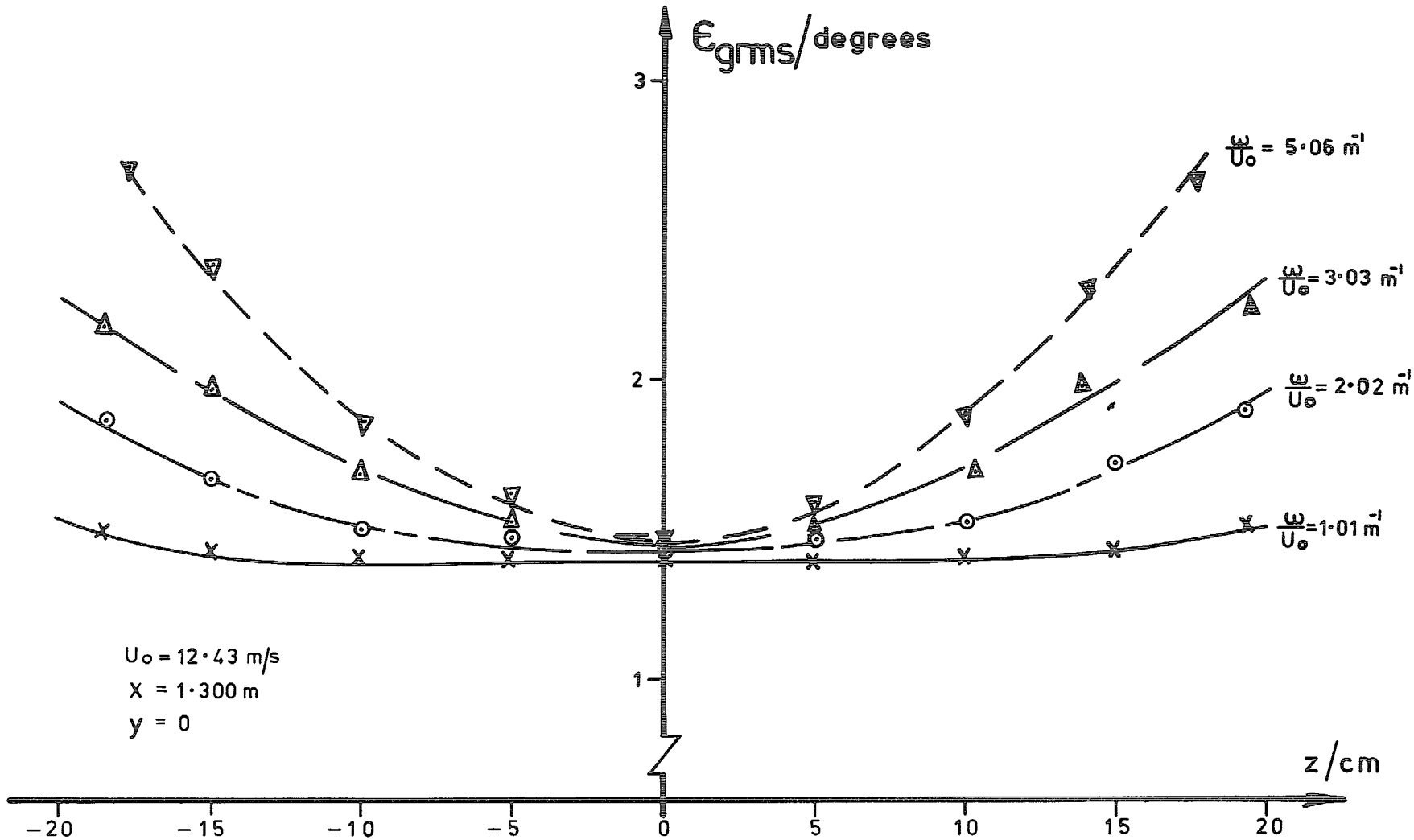

FIG. 19. Gust angle amplitude against vertical distance z.

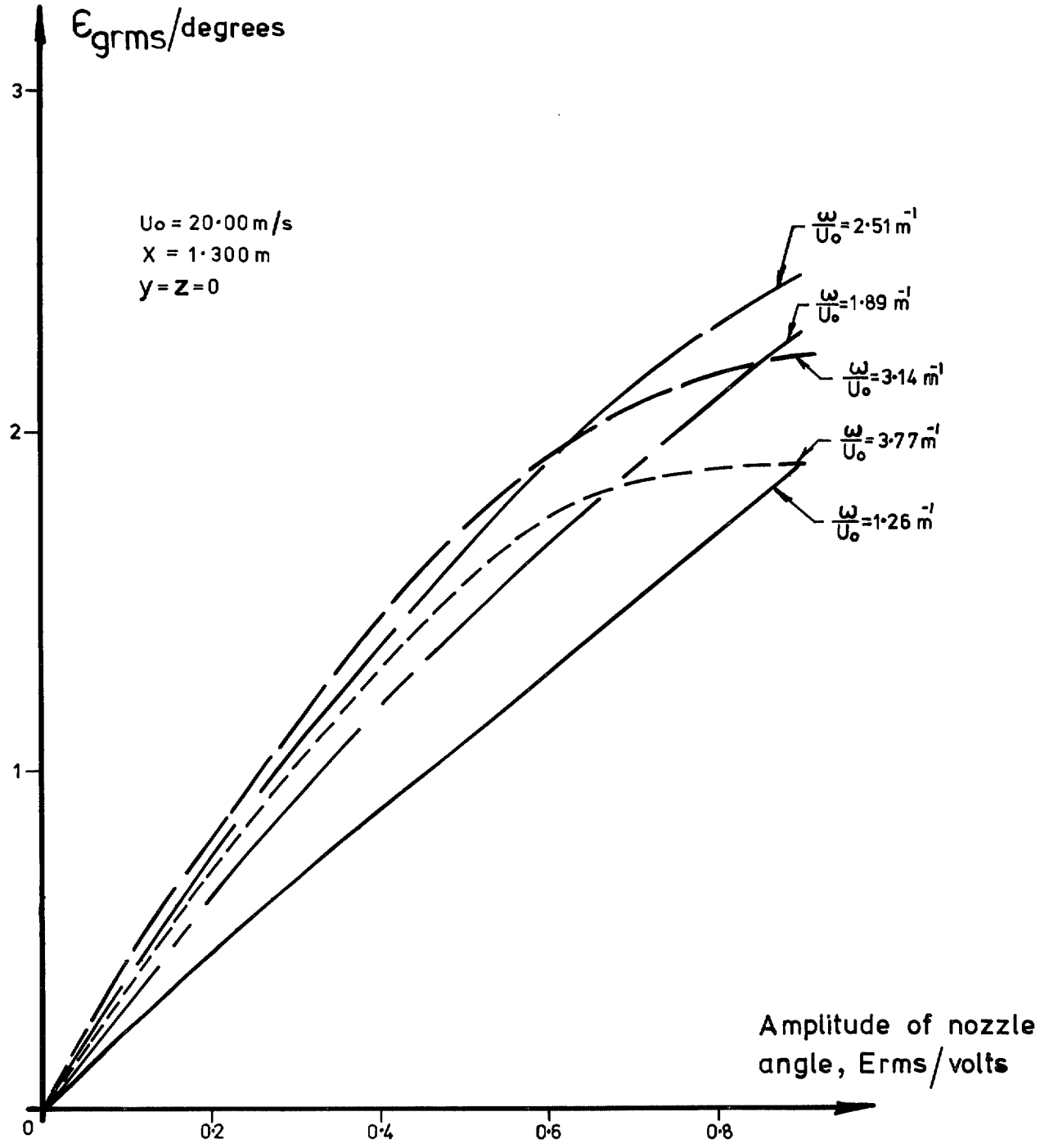

FIG. 20. Gust angle amplitude variation with amplitude of perturbing nozzle angle.

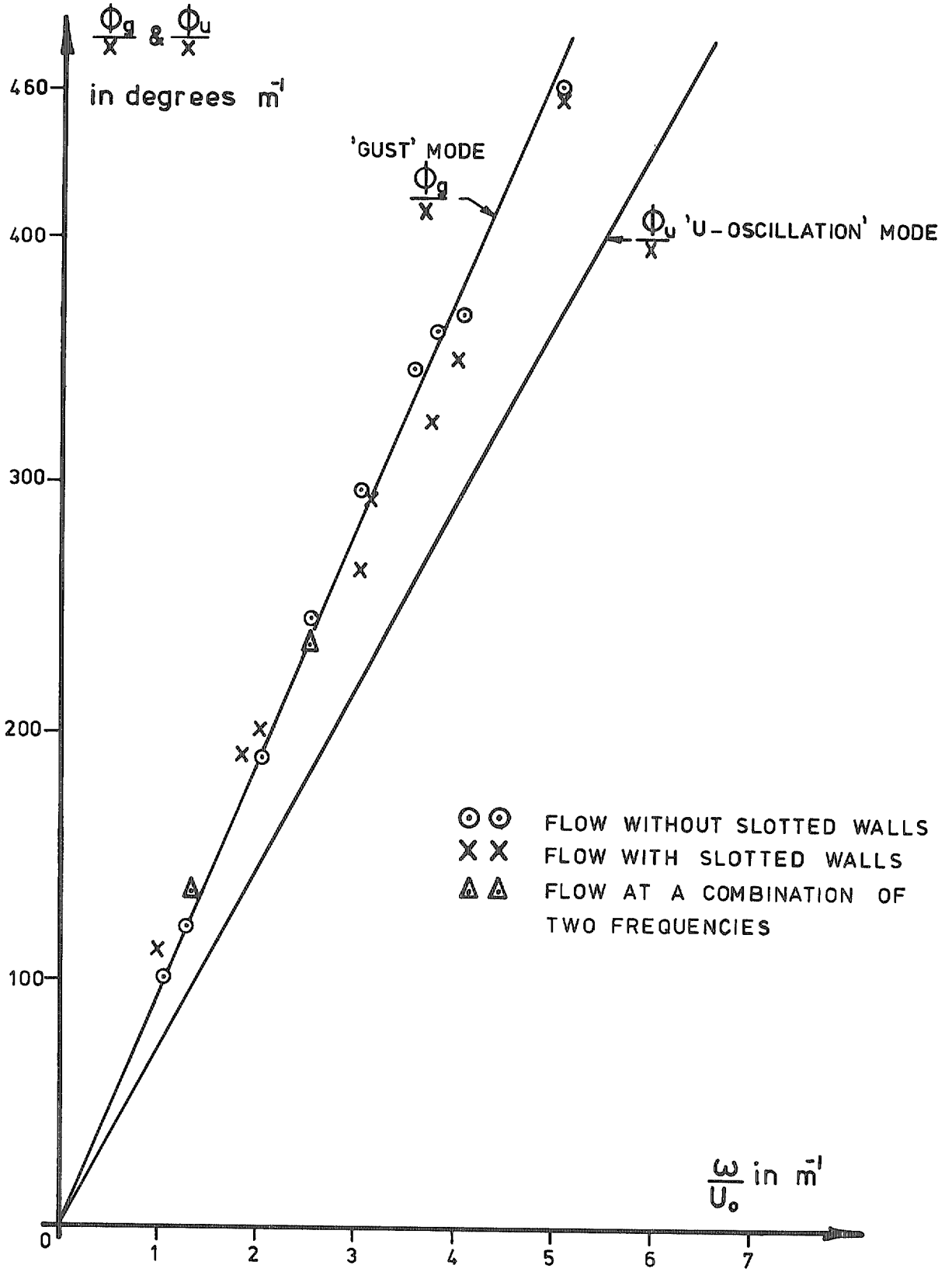

FIG. 21. Downstream phase lag/metre against frequency parameter/metre.

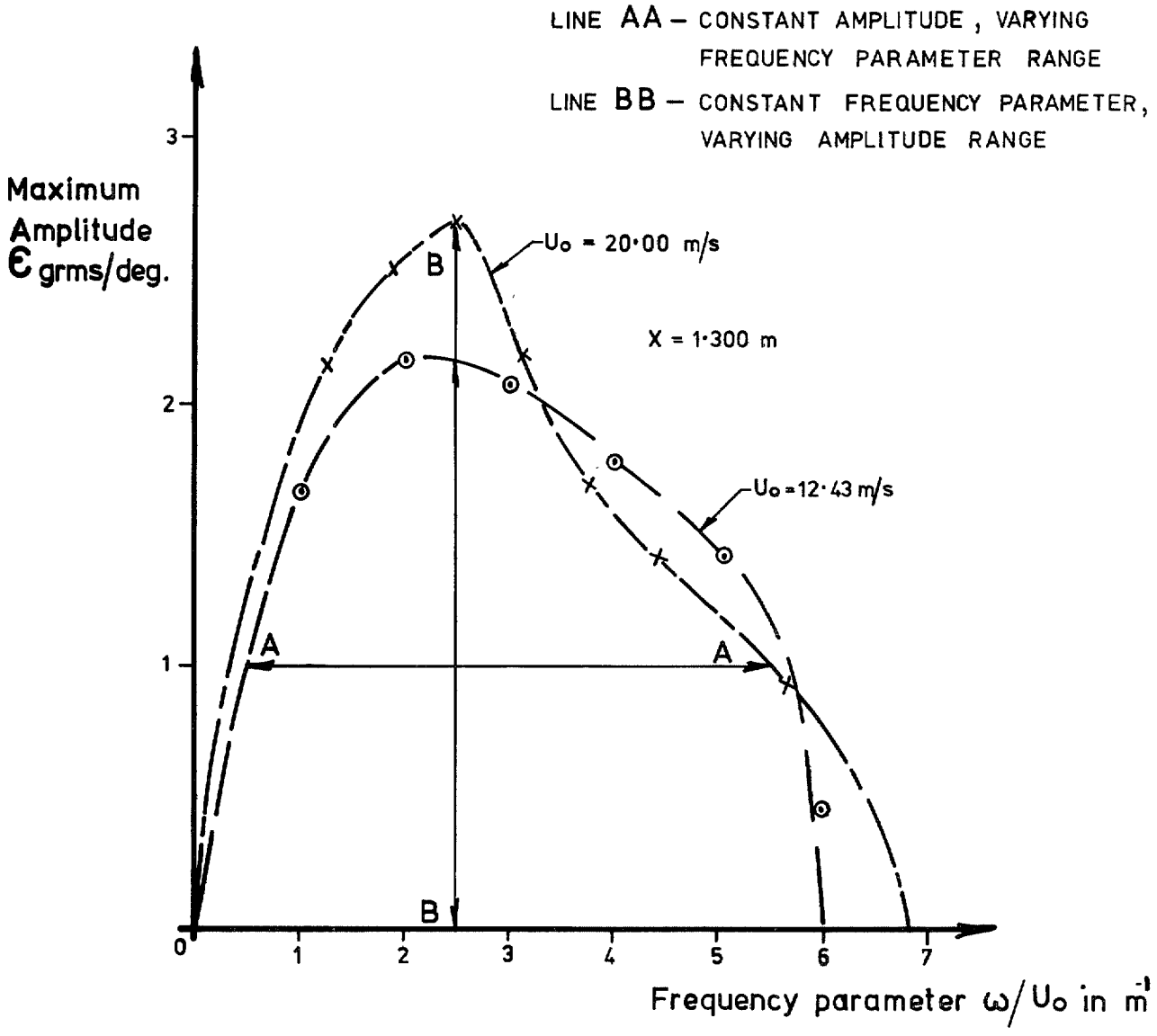

FIG. 22. Envelope of possible amplitude frequency combinations.

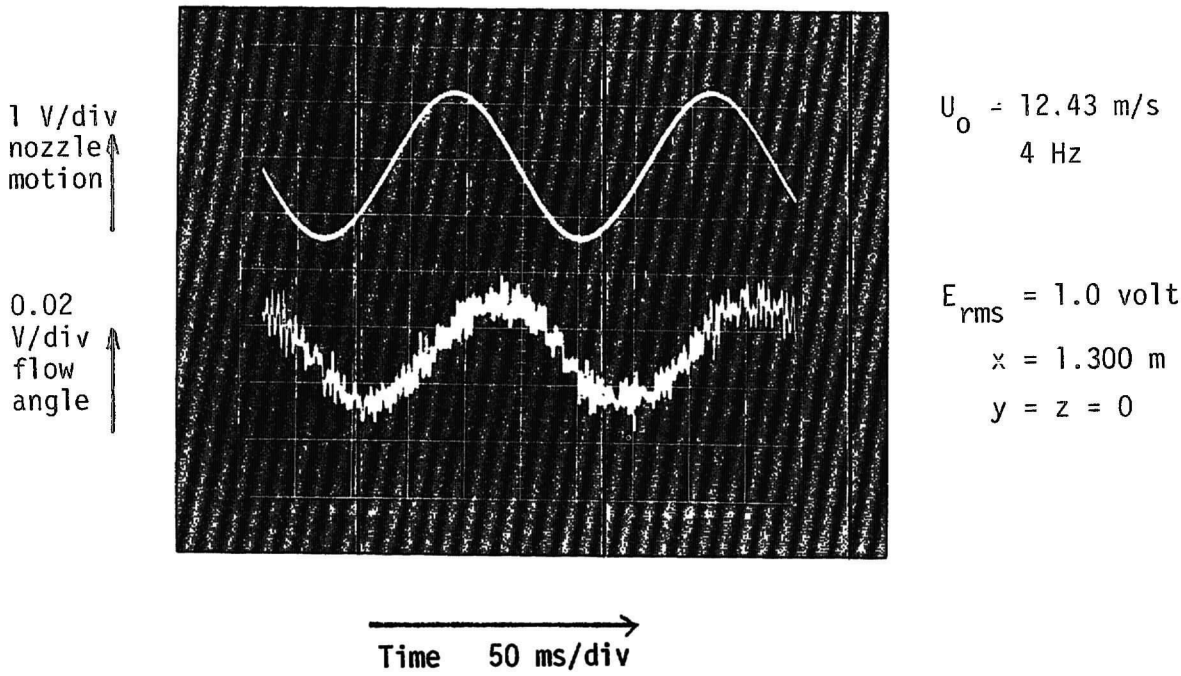

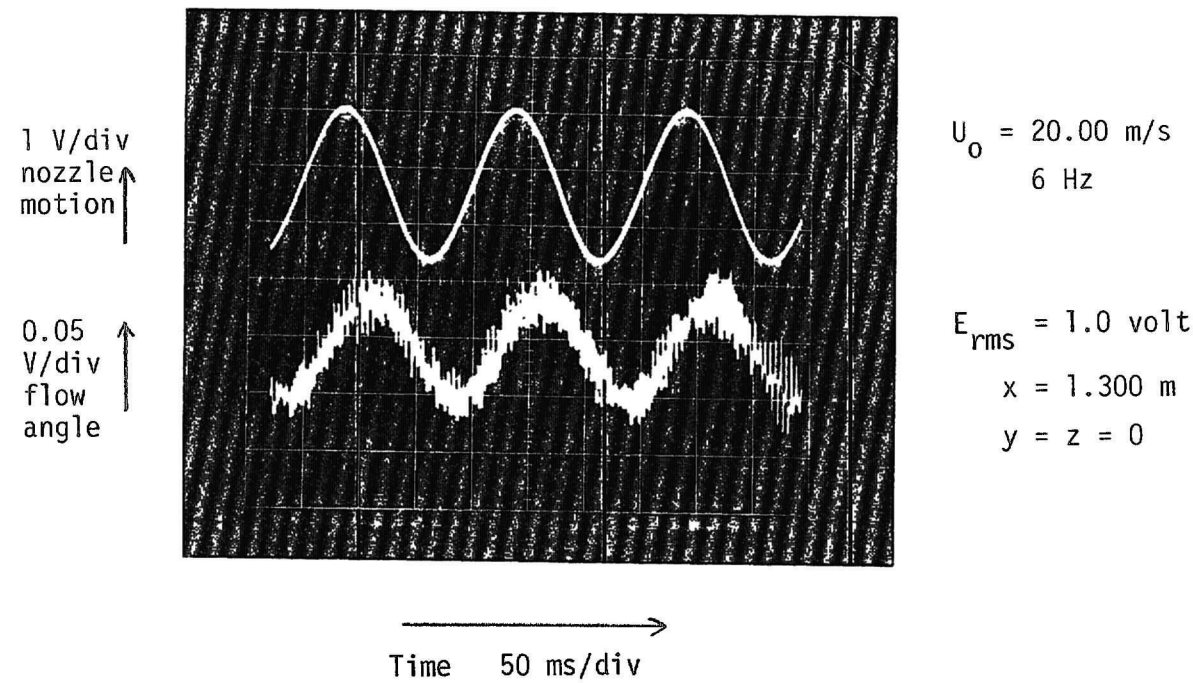

FIG. 23. Typical waveforms of nozzle motion and flow response in the gust tunnel.

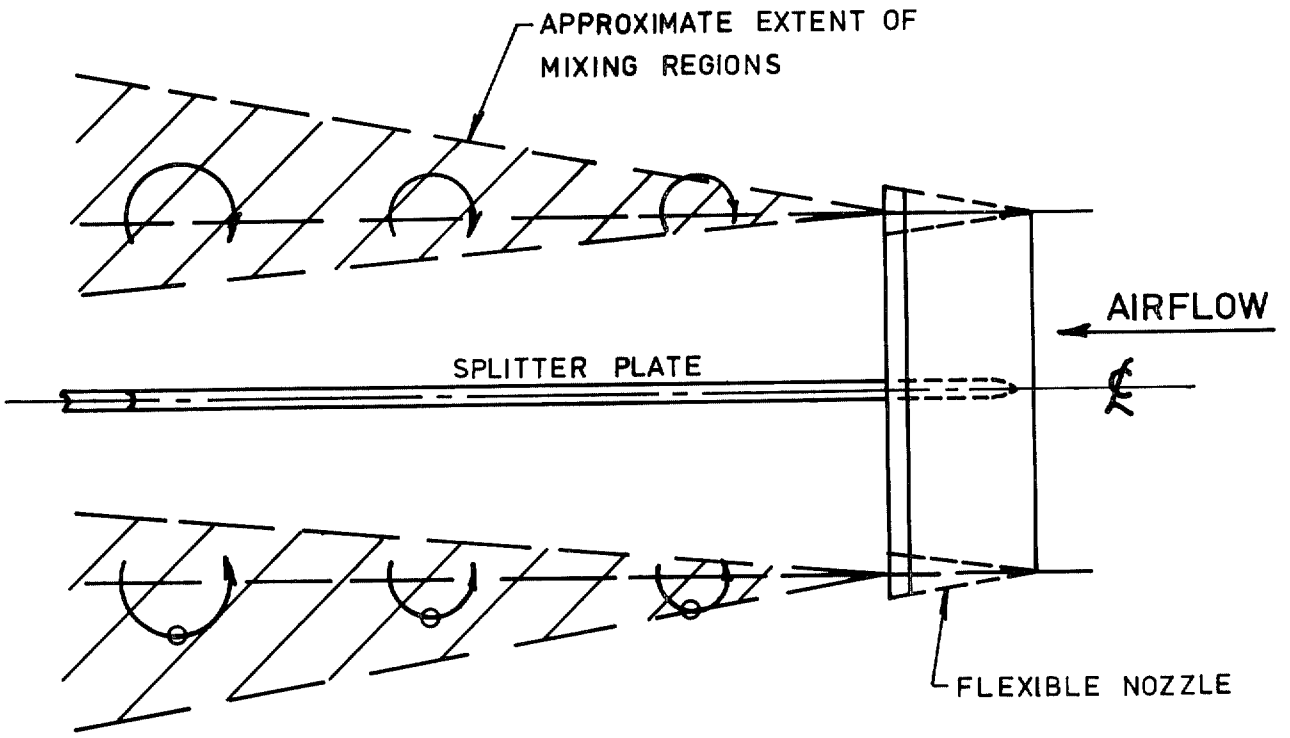

ROLLING UP VORTICES FROM
UPPER SHEAR LAYER

IMAGE VORTICES DUE TO PRESENCE
OF SPLITTER PLATE

FIG. 24. Flow field structure with splitter plate.

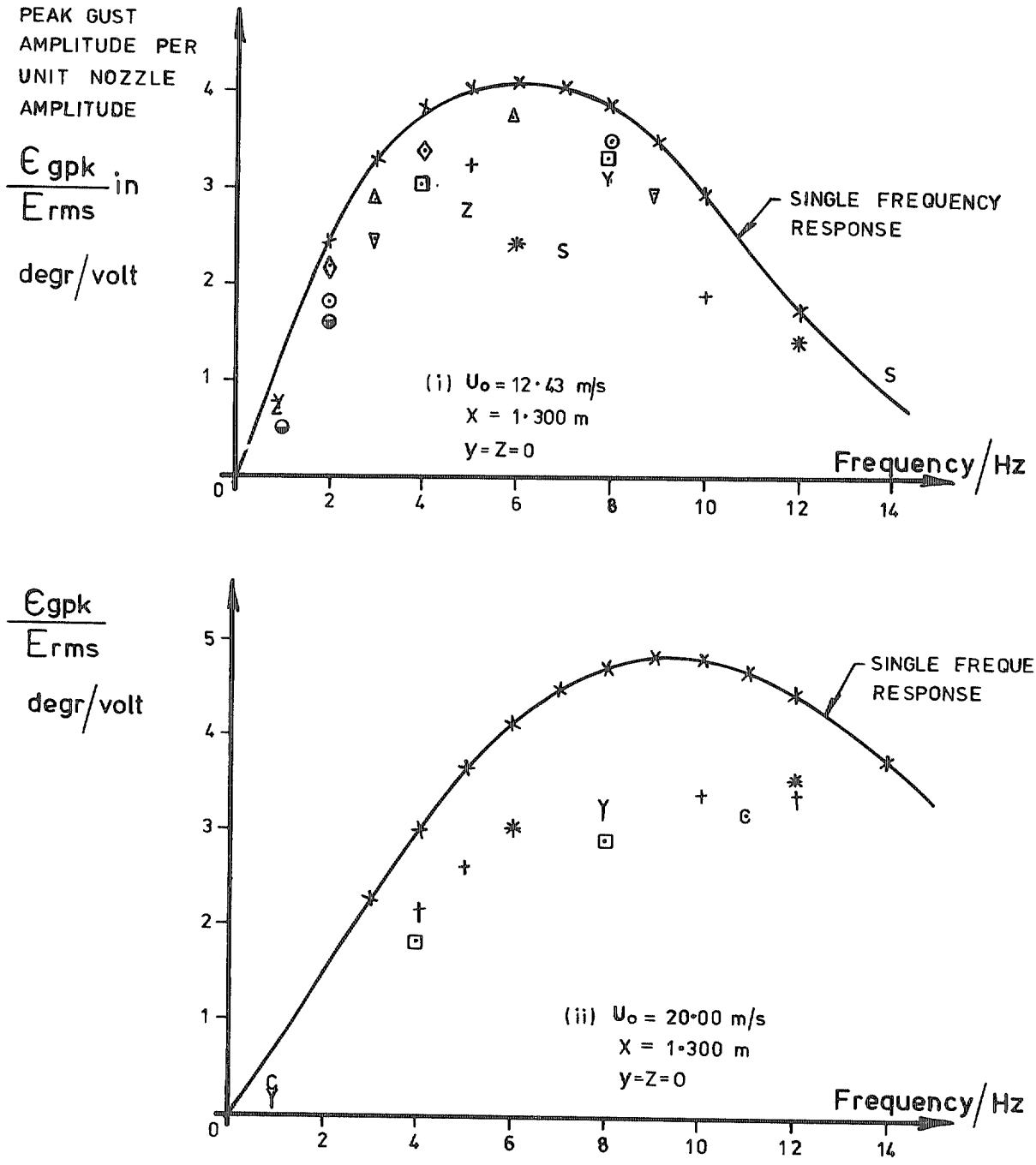

Each pair of points here plots the two components of the 'double frequency' response;
⊡ denotes the response at 4 and 8 Hz
✳ denotes the response at 6 and 12 Hz etc.

FIG. 25. Gust tunnel response to double frequency oscillatory inputs.

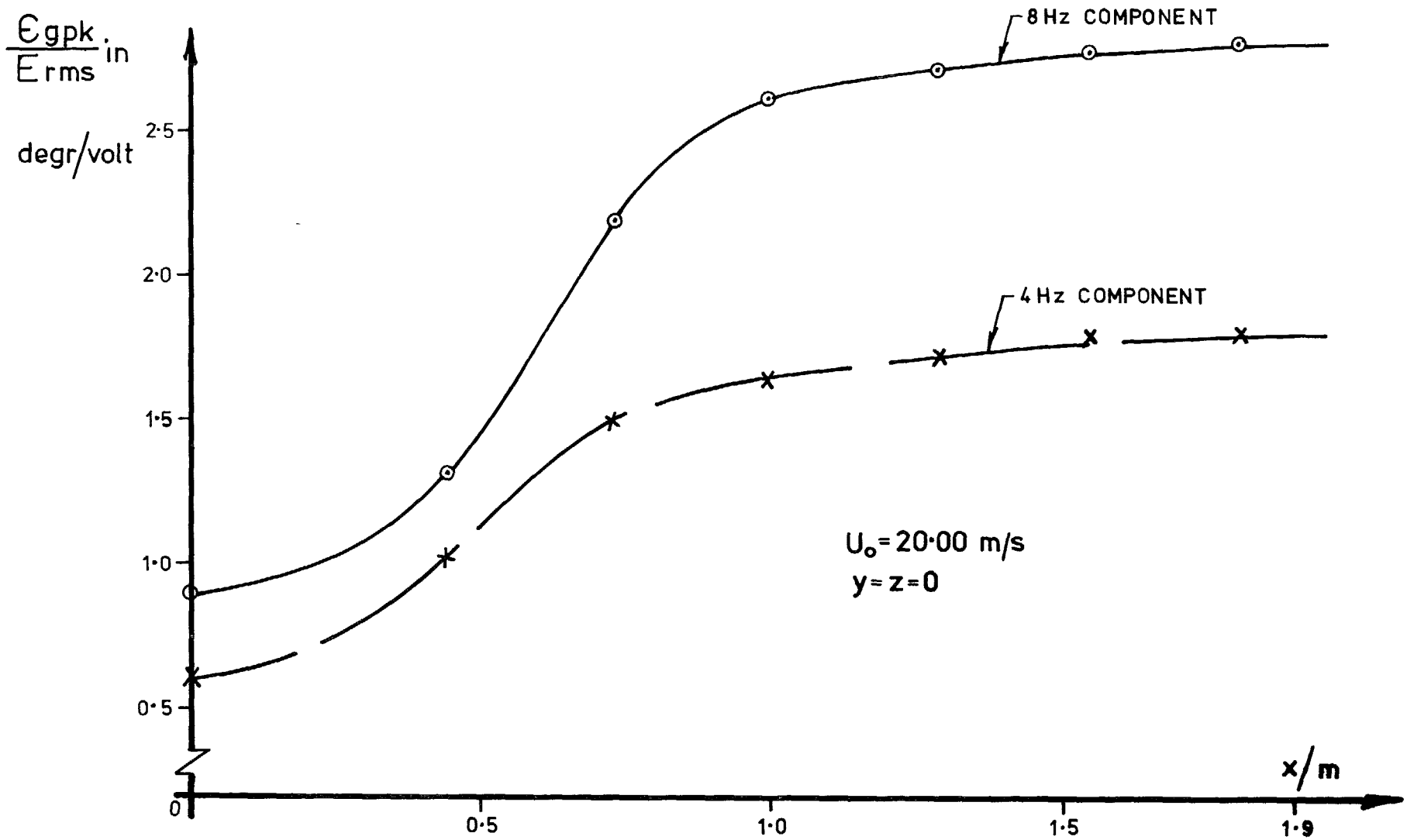

FIG. 26. Amplitude variation with x for response to double frequency excitation.

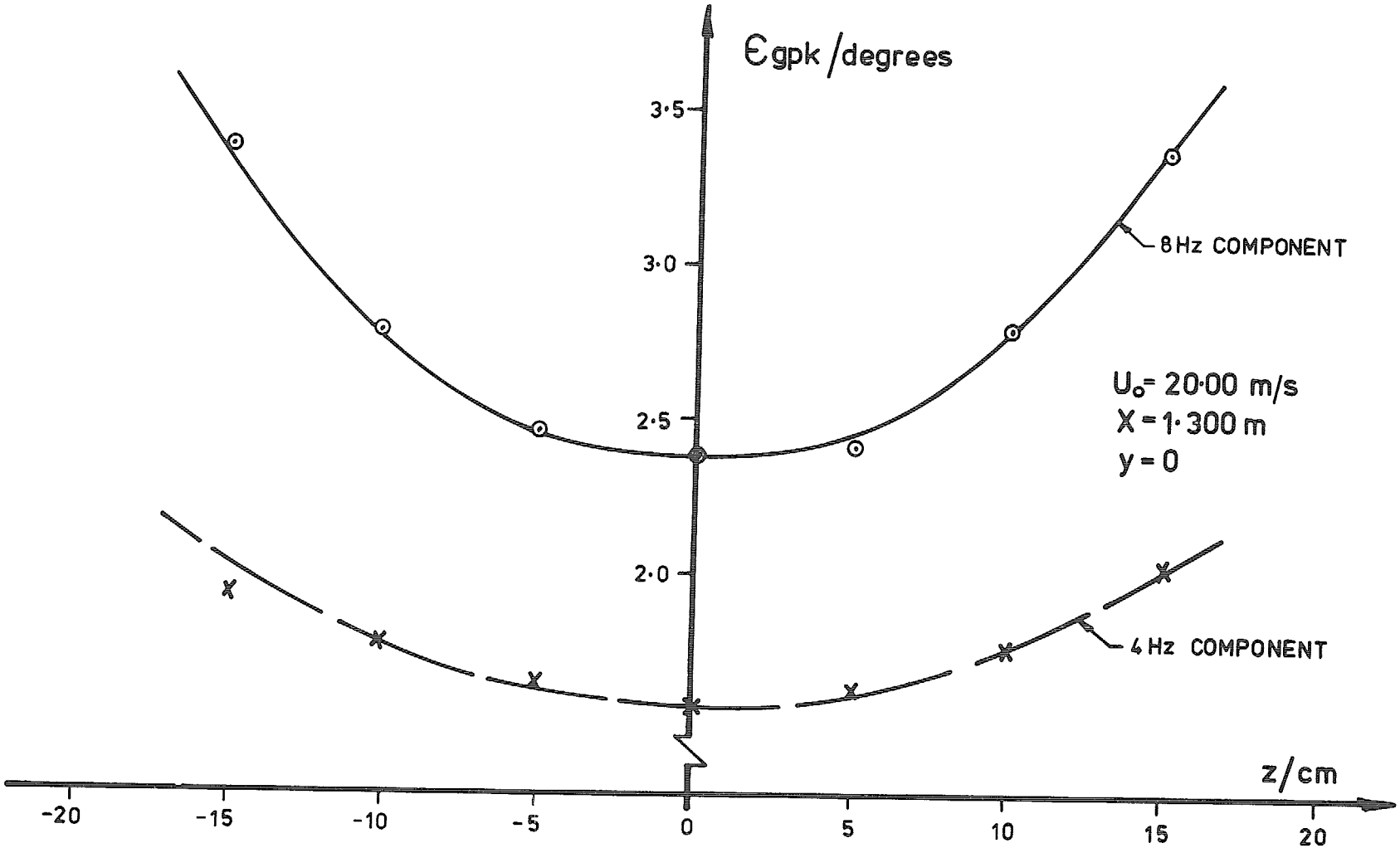

FIG. 27. Amplitude variation with z for double frequency excitation.

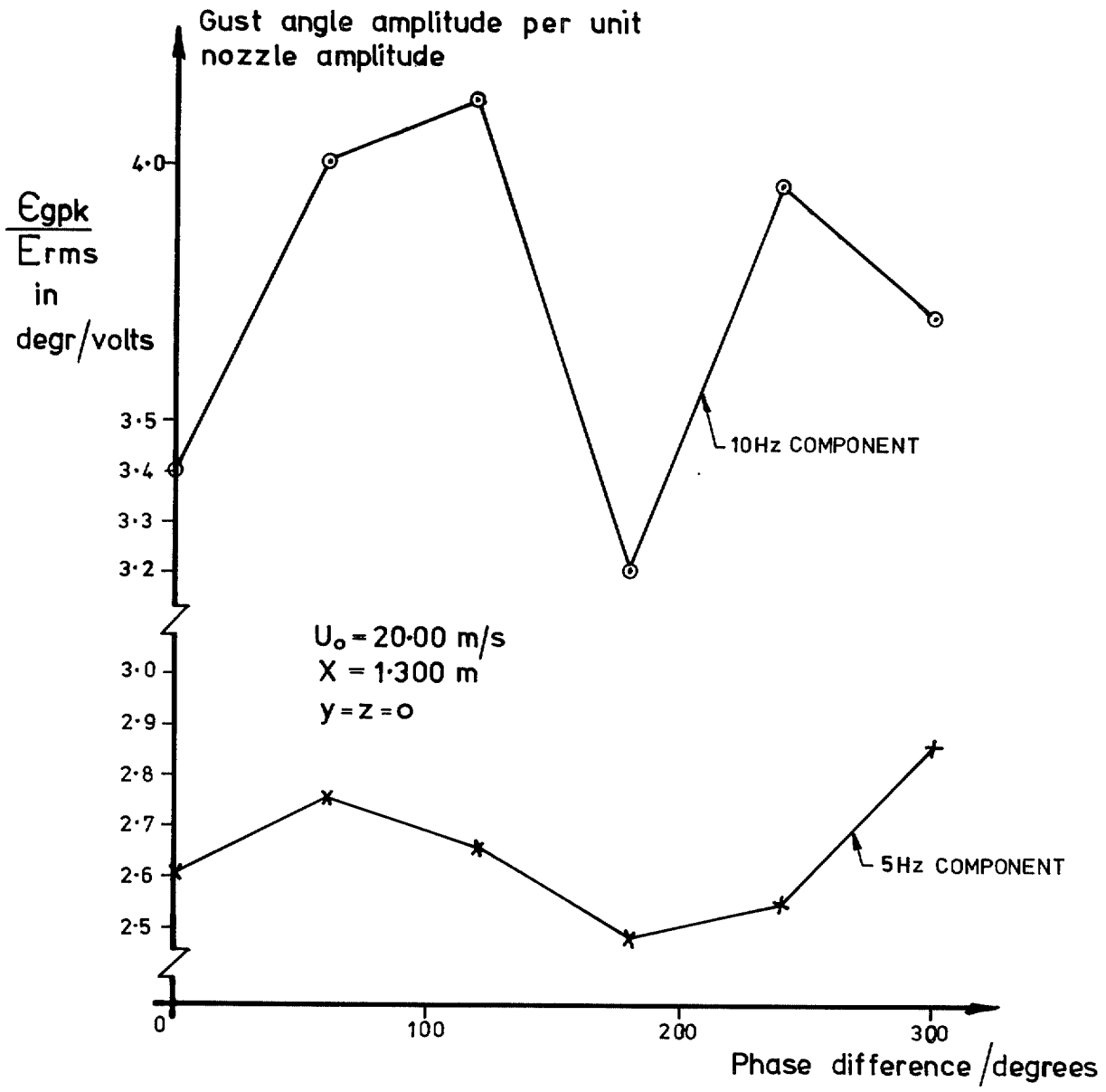

FIG. 28. Variation of flow response with phase difference between the two nozzle input frequencies.

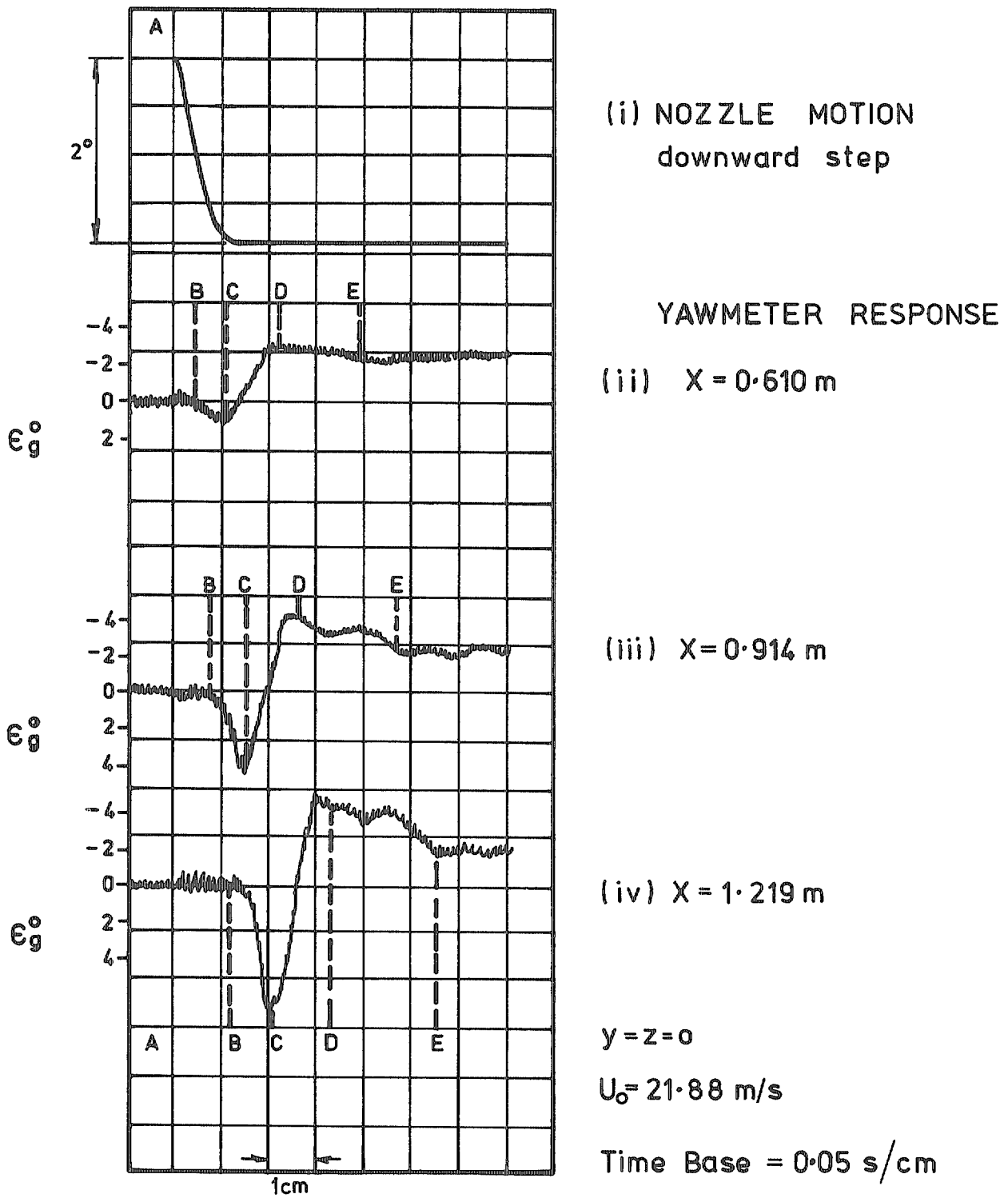

FIG. 29. Step input response (Parker[10]).

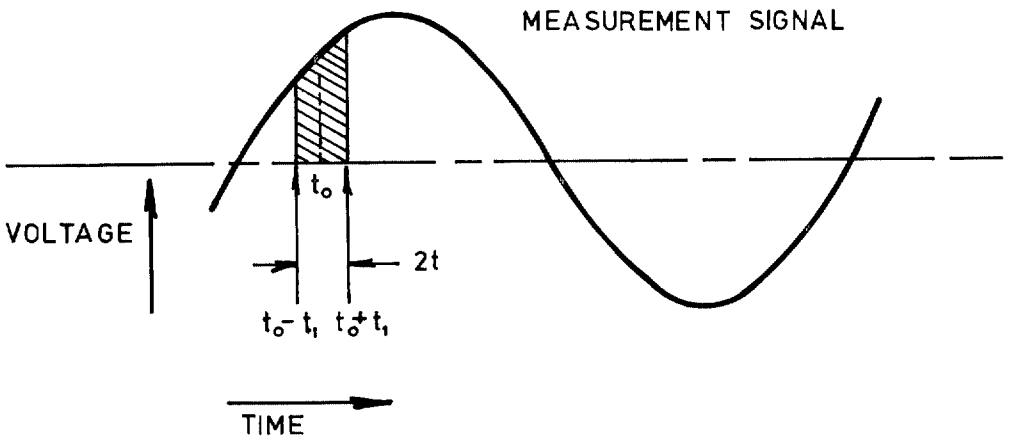

MEASUREMENT AVERAGED OVER SHADED AREA

t_o INSTANT AT WHICH MEASUREMENT IS REQUIRED

$2t_1$ DIGITAL VOLTMETER MEASUREMENT TIME — 20 milliseconds

FIG. 30. Effect of digital voltmeter measurement time.

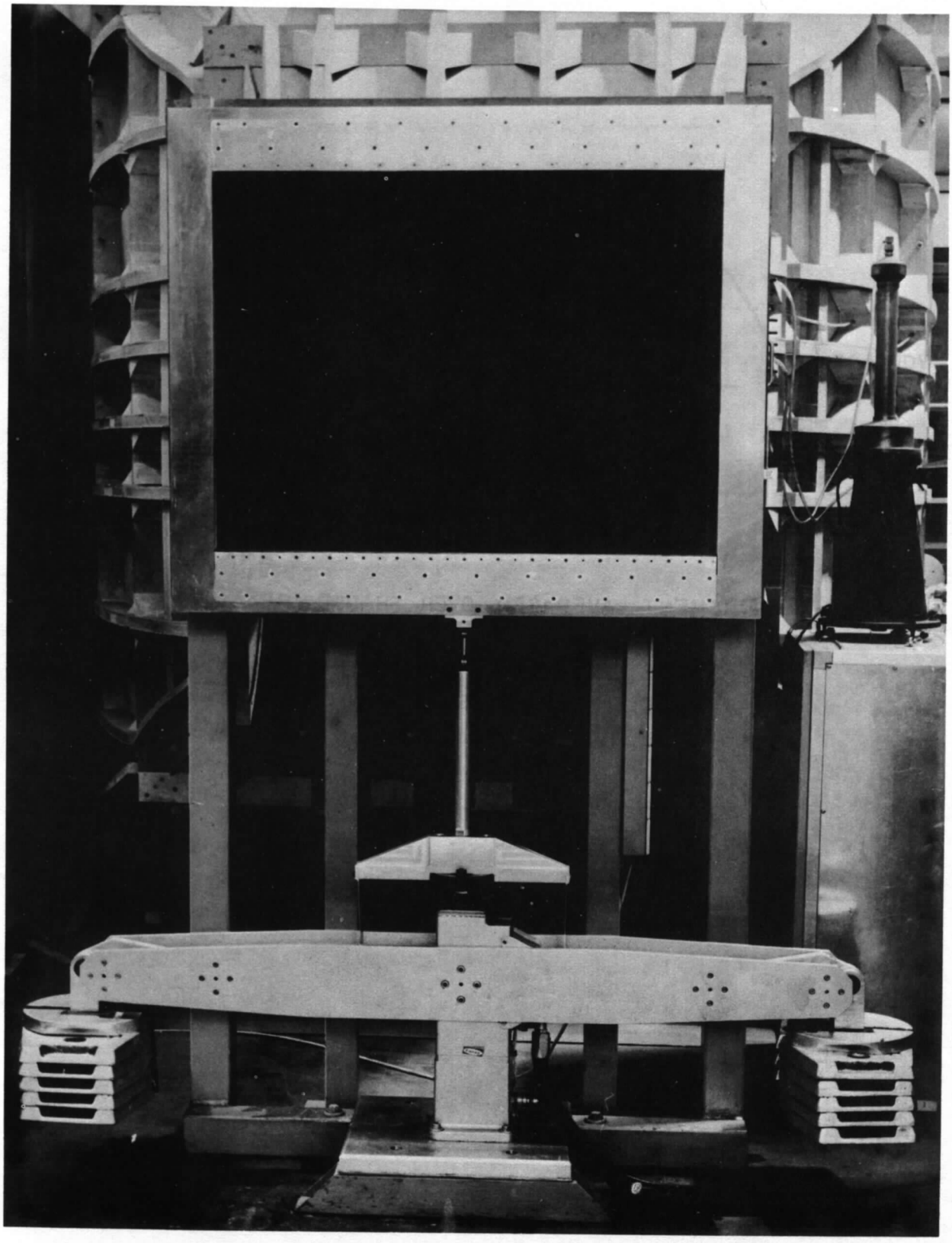

PLATE I. The flexible nozzle and actuating mechanism.

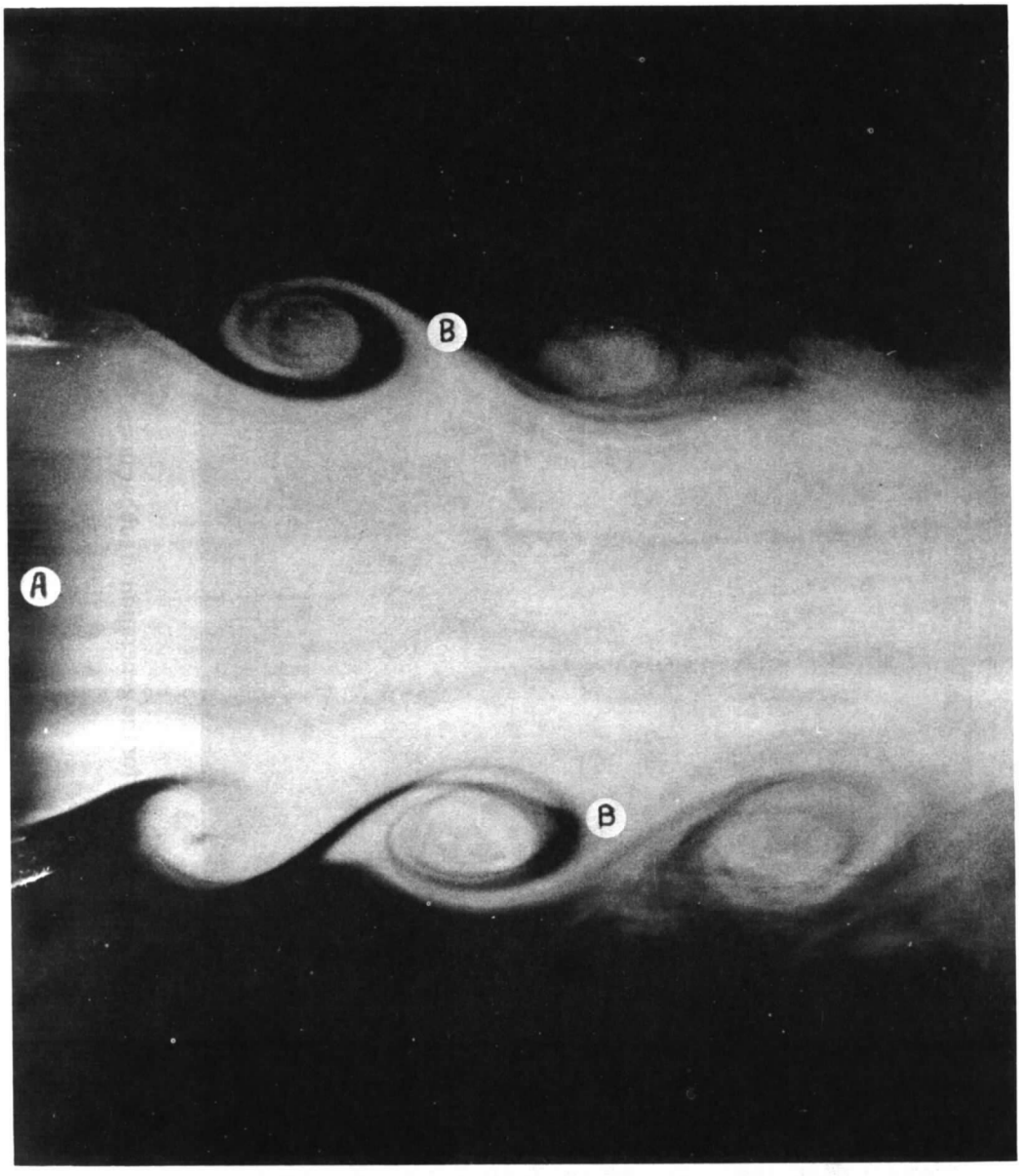

PLATE II. Flow visualisation test with smoke in a model of the gust tunnel.
A—nozzle exit.
B—upper and lower vortex streets convecting downstream.
Direction of flow is from left to right.

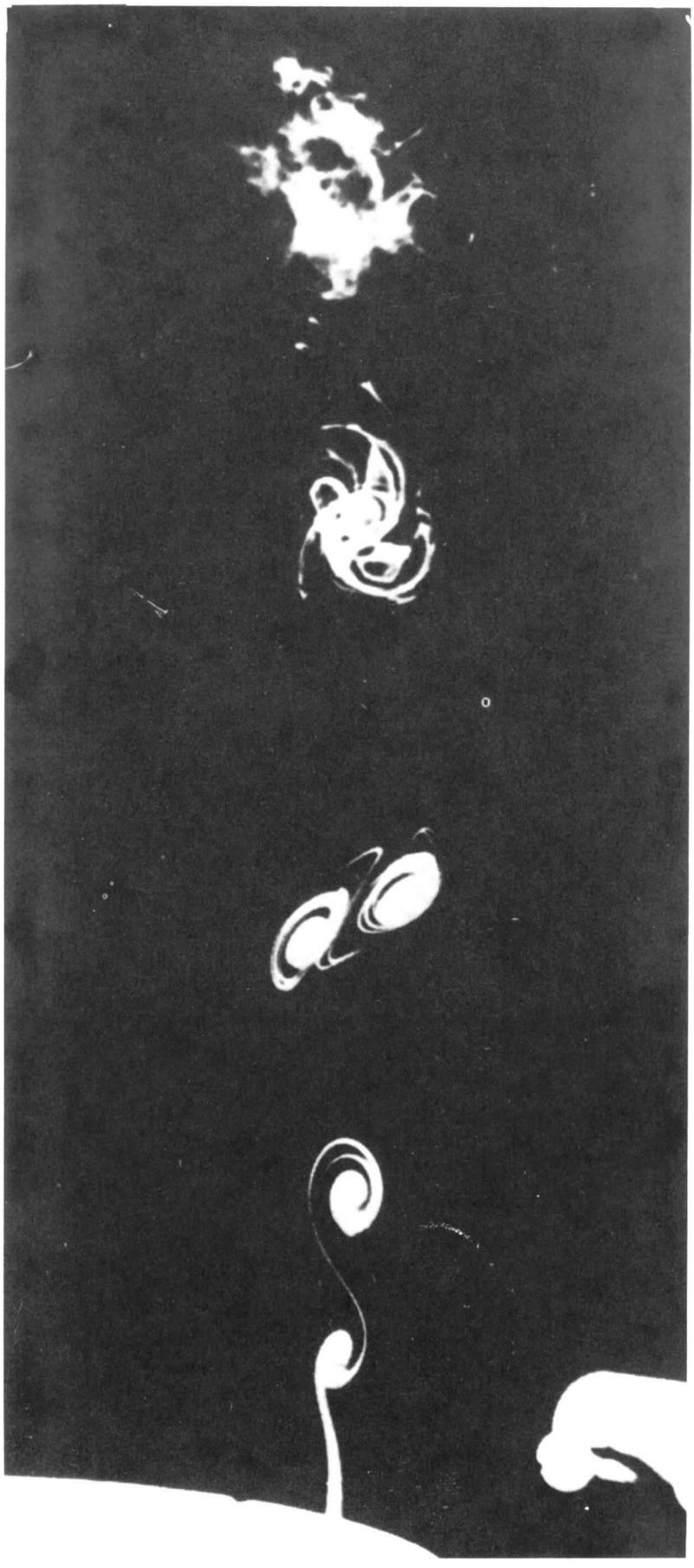

PLATE III. Flow visualisation result demonstrating the mechanism for the generation of subharmonic fluctuations (by Freymuth[12])

Printed in England for Her Majesty's Stationery Office by J. W. Arrowsmith Ltd., Bristol BS3 2NT
Dd. 587484 K.5. 6/77.

HER MAJESTY'S STATIONERY OFFICE

Government Bookshops

49 High Holborn, London WC1V 6HB
13a Castle Street, Edinburgh EH2 3AR
41 The Hayes, Cardiff CF1 1JW
Brazennose Street, Manchester M60 8AS
Southey House, Wine Street, Bristol BS1 2BQ
258 Broad Street, Birmingham B1 2HE
80 Chichester Street, Belfast BT1 4JY

Government publications are also available through booksellers

ISBN 0 11 470973 4